9-2016

Ricketts Analysis Using Conventional and DolphinTM Generated CBCT Lateral Cephs

Yeganeh Parhizkar Jewell

LOMA LINDA UNIVERSITY
School of Dentistry
In conjunction with the
Faculty of Graduate Studies

Ricketts Analysis
Using Conventional and Dolphin™ Generated CBCT Lateral Cephs

by

Yeganeh Parhizkar Jewell

A Thesis Submitted in partial satisfaction of
the requirements for the degree
Master of Science in Orthodontics and Dentofacial Orthodpedics

---

September 2016

Each person whose signature appears below certifies that this thesis in his opinion is adequate, in scope and quality, as a thesis for the degree Master of Science.

_____, Chairperson

V. Leroy Leggitt, Professor of Orthodontics and Orthopedics

_____

Joseph M. Caruso, Professor of Orthodontics and Dentofacial Orthopedics

_____

Kitichai Rungcharassaeng, Professor of Orthodontics and Dentofacial Orthopedics

ACKNOWLEDGEMENTS

Completion of this research project would have not been possible without the guidance of my committee members and the support from my family, husband, and friends.

I owe my deepest gratitude to the members of my committee who helped me accomplish and complete this thesis. I appreciate Drs. Leroy Leggitt, Kitichai Rungcharassaeng, and Joseph Caruso for all their advice and commentary throughout the progress of this thesis. I would also like to thank Dr. Udo Oyoyo for his help in formulating the statistics of this research project as well as Mr. Seth Myhre for his help in construction radiographic phantom and operation of the CBCT machine.

I would like to dedicate this thesis to my parents, Abdollah Parhizkar and Zohreh Barati, who believed in me and sacrificed so much to help support me throughout my education.

CONTENT

TABLES

Tables Page

FIGURES

Figures Page

ABBREVIATIONS

CBCT	Cone Beam Computed Tomography
2D	Two-Dimensional
3D	Three-Dimensional
PA	Periapical
TMJ	Temporomandibular joint
Na	Nasion
Or	Orbitale
P	Porion
FH	Frankfort horizontal
ANS	Anterior nasal spine
Po	Pogonion
Gn	Gnathion
Go	Gonion
Me	Menton
Ba	Basion
T1	Initial records
T2	Finishing records
VT	Total vertical
HT	Total horizontal
S ½ VT	Superior vertical half
I ½ VT	Inferior vertical half
L ½ HT	Left horizontal half
R ½ HT	Right horizontal half

MIP	Maximum intensity projection
I-I Angle	Interincisal angle
U1 Prot	Upper incisor protrusion
L1 Prot	Lower incisor protrusion
L1 to APo	Lower incisor to APo
U6 – PTV	Upper molar to PT Vertical
Mnd Arc	Mandibular Arc
MPA	Mandibular plane angle
Mx Depth	Maxillary depth
F-Axis	Facial axis
F-Depth	Facial Depth
C-Length	Cranial length
C-Def	Cranial deflection
LFH	Lower face height
LL-E	Lower lip to E-plane
N-Me	Nasion to menton
N-Ba	Nasion to basion

ABSTRACT OF THE THESIS

Ricketts Analysis
Using Conventional and Dolphin™ Generated CBCT Lateral Cephs

by

Yeganeh Parhizkar Jewell

Master of Science
Graduate Program in Orthodontics and Dentofacial Orthopedics
Loma Linda University, September 2016
Dr. V. Leroy Leggitt, Chairperson

Purpose: The aim of this study was to evaluate the difference between Ricketts analysis measurements made on Sirona Orthophos XG Plus (Sirona Dental Systems, Charlotte,NC) lateral cephalograms, and Dolphin™ generated perspective and orthogonal lateral cephalograms from CBCT (NewTom 5G; QR srl, Verona, Italy).

Materials and Methods: A Sirona digital lateral cephalogram and Dophin™ synthesized CBCT lateral cephalograms of a radiographic phantom in orthogonal and perspective projections were created. Horizontal and vertical measurements were made in multiple planes on the radiographic phantom to compare each imaging modality.

Twenty-five lateral cephalometric radiographs were selected retrospectively from the records of patients of the LLUSD Graduate Orthodontic Clinic who had both CBCT and Sirona digital lateral cephalograms. Radiographs were excluded from the study if they displayed significant occlusal plane discrepancy (>2 mm), or missing first molars. All lateral cephalograms were digitized into Dolphin™ (version 11.8; Dolphin Imaging & Management Solutions, Chatsworth, Calif) and traced using Ricketts cephalometric analysis in addition to measurements from Nasion to Menton and Nasion to Basion. Eight

linear and nine angular measurements from each imaging modality were compared and analyzed using one sample Wilcoxon signed rank test and pairwise comparison.

Results: Statistically significant differences were found in percent magnification of horizontal and vertical measurements between the scanned grid and the various imaging modalities. No significant single plane perspective distortion (SPPD) was detected in the vertical and horizontal directions. Multiplane perspective distortion (MPPD) was only noted in Sirona images.

Ricketts Analysis linear measurements were all statistically different except for lower lip to E-plane ($P = 0.544$). The Ricketts Analysis angular measurements were not statistically different ($P < 0.05$) with the exception of facial axis ($P = 0.004$) and maxillary depth ($P = 0.025$). Dolphin^{TM} generated CBCT lateral cephalograms with orthogonal projection, adjusted to 101% magnification had the closest agreement to Sirona images.

Conclusions: No clinically significant perspective distortion was found in the vertical and horizontal direction in the three modalities that were studied. Dophin^{TM} synthesized CBCT lateral cephalogram in perspective projection does not produce perspective images. CBCT Lateral cephalograms generated by Dophin^{TM} in orthogonal projection at 101% magnification is compatible with images from Sirona for clinical evaluation.

CHAPTER ONE

REVIEW OF LITERATURE

Since the introduction of cephalostat by Broadbent in 1931, cephalometry has been commonly used by orthodontists.[1] A significant portion of diagnostic assessment of skeletal and dental problems, and evaluation of treatment progress in orthodontic patients is dependent on radiographic images. Cephalometric analysis requires identifying specific landmarks and calculation of multiple angular and linear measurements. These measurements are then compared to normal values that have been obtained from two dimensional (2D) cephalograms based on different age, sex and ethnical groups. Cephalometric radiographs have a number of limitations. Just like any other transmission radiographs, lateral cephalometric radiographs collapses a three-dimensional (3D) structure into a two-dimensional plane. This results in difficult landmark identification especially for bilateral structures. Furthermore, due to non-parallel x-ray projection, the structures that are more proximal to the x-ray source appear more magnified than those proximal to the detector. Moreover, patient positioning in lateral cephalograms limits the ability of reproducing and superimposition of consecutive images. These three factors alone can cause significant variation on cephalometric measurements.[2]

From the beginning Broadbent stressed the importance of combining the lateral and postero-anterior head films to have more than a 2D image of the skull. In most cases however this principal is not used in orthodontic practice. In 1998, Cone beam computed tomography (CBCT) was developed specifically for imaging the structures relevant to dentistry.[3] CBCT imaging has specially been valuable in TMJ studies, implant placements, orthognathic surgeries, and cases with impacted teeth.[4-7] One of the main

advantages of current CBCT machines lies in their reduced radiation dose compared to CT.[8] The radiation dose to the patient with CBCT is 40% less than conventional CT and 3 to 7 times more than panoramic doses.[9] Therefore, conventional images still delivers lowest doses to patient. One needs to keep in mind that the CBCT does varies substantially depending on the device, field of view (FOV), and selected technique factors.[10]

Because of the advantages and possibilities of CBCT more orthodontists are using it routinely for orthodontic patient assessment. In the near future, as the radiation dose of CBCT diminishes, it may replace conventional 2D imaging. However, in order to be able to use previously collected data that was based on conventional cephalograms, a way of comparing the two should be established. Furthermore, a proper diagnosis in orthodontics leads to logical treatment plan which needs to be evaluated and revised as necessary as the treatment progresses.[11] Since CBCT radiation doses have not reached that of conventional imaging, it is not recommended to be used for treatment progress evaluation. Therefore, if initial records are taken by CBCT, an orthodontist needs to be able to directly compare subsequent progress records taken by conventional techniques to that of CBCT. Luckily, 2D images can be synthesized from CBCT 3D data and these synthesized images may bridge the gap between 2D and 3D. Current literature is focused on the compatibility of conventional cephalograms and CBCT synthesized cephalograms and their similarity and/or difference in magnification, distortion, and landmark identification.

In general, when comparing cephalometric measurements between conventional and CBCT derived lateral cephalograms, differences in linear measurements are greather

than angular measurements.[12-17] In a study by Kumar et al.,[12] a sample of ten dry skulls were imaged by both conventional cephalometry (Wehmer cephalostat) and CBCT (NewTom 3G). Orthogonal cone bean CT projection with no magnification and perspective projection with 7.5% simulated magnification were obtained. Differences between the modalities were found not to be statistically significant except for the mandibular unit length (Go-Gn). When the midsagittal linear measurements were compare to the actual skull measurements however, conventional imaging was found to underestimates the actual skull dimensions while the perspective CBCT overestimated the skull dimensions. Furthermore, orthogonal CBCT was found to provide measurements that were closest to the actual measurements. In a vivo study of thirty-one patients, kumar et al.,[13] compared angular measurements and found no significant differences in angular measurements in orthogonal, perspective and conventional lateral cephalometry with the exception of the Frankfort-mandibular angle. Lamichane et al.,[14] used a radiographic phantom and found that perspective lateral cephalograms from CBCT could replicate the inherent magnification of a conventional lateral cephalograms with high accuracy, and that the measurements on the orthogonal projections were closer to the actual measurements. Park et al.,[15] however found statistical differences in linear measurements for U1 to facial plane distance and angular differences in gonial angle, ANB difference, and facial convexity. Hilger et al.,[16] also found all CBCT measurements to be accurate close to anatomical truth, however LC measurements of condylar length, condylar height, and lateral pole of gonion were different from the anatomic truth by 2.28 mm (25.9%), 1.97 mm (10.1%) and 8.99 mm (17.5%) respectively. Moshiri et al.,[17] found that nine linear measurements conventional lateral cephalograms were accurate for

Po-Or and ANS-N measurements, whereas CBCT images were accurate for all the measurements except Pog-Go, and Go-Me.

Unlike two dimensional cephalometric norms, no three dimensional standards from large untreated population analyzed by way of 3D examinations are available today. In a study by Gribel et al.,[18] authors opted to test a mathematical model to convert the normal values of 2D lateral films into 3D measurements. Using the algorithm stated in their article, they were able to correct for both magnification and image distortion (mean difference of 0.1mm) between CBCT and lateral films. Authors suggest that this simple algorithm can be used to convert existing cephalometric growth studies into 3D normal values without further radiation of untreated subjects.

Landmark identification is one of the major areas of error in tracing. In most cases this error is related to specific landmarks which may be harder to identify. Generally higher errors are associated with 2D imaging.[19,20] Intraexaminer and interexaminer reliabilities in landmark identification was studied by Lagrave et al.,[19] on a sample of 10 adolescent patients on the x,y, and z coordinates. Intraexaminer and interexaminer reliabilities for the x, y, and z coordinates for all landmarks in CBCT were greater than 0.9. Intraexaminer and interexaminer of most landmarks in the lateral cephalograms were greater than 0.9, except porion, basion, and condylion had moderate intraexaminer reliability for the x-axis and mild interexaminer reliability for the y-axis.

In 2009 Chien et al.,[20] also studied the difference in landmark identification in vivo. Errors were generally larger in 2D rather than 3D. Two dimensional images also have more errors that were greater than 1mm and included A-point, ANS, basion, condylion,

L6 occlusal, midramus, orbital, porion, ramus point and sigmoid notch. The errors in 3D that were greater than 1mm were the condylion, orbital, gonion, and midramus.

Landmark identification has been studied in a number of researches.Change et al.,[21] compared landmark identification in conventional lateral cephalograms and CBCT derived cephalograms. In this study, image modality was not the significant variable in the final generalized estimating equations model. The regression coefficient estimates of the significant landmarks for the overall identification error ranged from −0.99 (Or) to 1.42 mm (Ba). The difficulty of identifying landmarks on structural images with multiple overlapping such as Or, U1R, L1R, Po, Ba, UMo, and LMo, increased the identification error by 1.17 mm, and some of them, including ANS, A, B, Go, Ba, and PNS, reached error close to clinical significance (0.5 mm). In the CBCT modality, the identification errors significantly decreased at Ba (−0.76 mm).

Delamer et al.,[22] studied a programme of professional calibration (PPC) that provided a lecture of cephalometric analysis presented by a PhD graduate in oral radiology and specialist in orthodontics and practical discussion session on cephalometric landmark identification. Authors concluded that a PCC was more influential in reduction of variability than type of imaging used. Yu et al.,[23] also found significant difference between observers in identifying landmarks such as porion, pogonion and R1. Cattaneo et al.,[24] also compared cephalometric measurements made on CBCT-synthesized lateral cephalograms in orthogonal projection and conventional cephalograms using Bjork analysis. In this study the influence of two different techniques used to obtain CBCT-synthesized lateral cephalograms, maximum intensity projection (MIP) and RayCast,

were also evaluated. They found that measurements did not differ between the three imaging techniques.

Damstra et al.,[25] used a midsagittal approach to position the bilateral structures by indicating a point on the midsagittal plane where a line joining the left and right anatomical structures met. Ten human skulls were used in which anatomical landmarks were marked by spherical metal markers. They found no significant difference between the two and three-dimensional measurements.

The findings of this review cannot be directly compared to each other due to large number of variables. The CBCT machine and software used to generate images need to be accounted for, thus the results cannot be extrapolated to all available CBCT machines and imaging softwares.

CHAPTER TWO

RICKETTS ANALYSIS USING CONVENTIONAL AND DOLPHIN™ GENERATED CBCT LATERAL CEPHS

Abstract

Purpose: The aim of this study was to evaluate the difference between Ricketts analysis measurements made on Sirona Orthophos XG Plus (Sirona Dental Systems, Charlotte,NC) lateral cephalograms, and Dolphin™ generated perspective and orthogonal lateral cephalograms from CBCT (NewTom 5G; QR srl, Verona, Italy).

Materials and Methods: A Sirona digital lateral cephalogram and Dophin™ synthesized CBCT lateral cephalograms of a radiographic phantom in orthogonal and perspective projections were created. Horizontal and vertical measurements were made in multiple planes on the radiographic phantom to compare each imaging modality.

Twenty-five lateral cephalometric radiographs were selected retrospectively from the records of patients of the LLUSD Graduate Orthodontic Clinic who had both CBCT and Sirona digital lateral cephalograms. Radiographs were excluded from the study if they displayed significant occlusal plane discrepancy (>2 mm), or missing first molars. All lateral cephalograms were digitized into Dolphin™ (version 11.8; Dolphin Imaging & Management Solutions, Chatsworth, Calif) and traced using Ricketts cephalometric analysis in addition to measurements from Nasion to Menton and Nasion to Basion. Eight linear and nine angular measurements from each imaging modality were compared and analyzed using one sample Wilcoxon signed rank test and pairwise comparison.

Results: Statistically significant differences were found in percent magnification of horizontal and vertical measurements between the scanned grid and the various

imaging modalities. No significant single plane perspective distortion (SPPD) was detected in the vertical and horizontal directions. Multiplane perspective distortion (MPPD) was only noted in Sirona images.

Ricketts Analysis linear measurements were all statistically different except for lower lip to E-plane ($P = 0.544$). The Ricketts Analysis angular measurements were not statistically different ($P < 0.05$) with the exception of facial axis ($P = 0.004$) and maxillary depth ($P = 0.025$). Dolphin™ generated CBCT lateral cephalograms with orthogonal projection, adjusted to 101% magnification had the closest agreement to Sirona images.

Conclusions: No clinically significant perspective distortion was found in the vertical and horizontal direction in the three modalities that were studied. Dophin™ synthesized CBCT lateral cephalogram in perspective projection does not produce perspective images. CBCT Lateral cephalograms generated by Dophin™ in orthogonal projection at 101% magnification is compatible with images from Sirona for clinical evaluation.

Introduction

Since the introduction of the cephalometer by Broadbent in 1931, cephalometric analysis has become a standard diagnostic method in the field of orthodontics and dentofacial orthopedics. Growth and treatment changes can be evaluated accurately only by obtaining sequential cephalograms. [1, 26] Three dimensional (3D) imaging technique are becoming increasingly popular and have opened new possibilities for orthodontic diagnosis and treatment assessment. [3] Although CBCT scans provide abundant information, conventional two dimensional (2D) lateral cephalograms are still used by most clinicians. Most importantly, these images are necessary for comparison to earlier databases. Additionally, since the radiation dose of most current CBCT machines is still higher than conventional imaging, the use of CBCT to obtain progress records is not feasible. [9,10]

Sources of Cephalometric Error in Conventional Digital Cephalograms

Landmark identification in cephalometric analysis has been studied in a number of published articles. In general, some landmarks are more reproducible than others and each landmark has been identified to have a characteristic envelope of error. In the literature, the magnitude of the clinical significance for cephalometric measurements varies but is usually regarded as a difference of less than 1 or 2 measuring units, while some authors have suggested that a difference of up to 5% is clinically acceptable.[27-29] With more recent methods of radiography, an average error of 0.6 mm on the xy coordinate represents a clinically acceptable level of accuracy.[2]

Patient head positioning is also one of the contributors to error in radiography. Lee et al.,[30] evaluated the effect of cephalometer misalignment on posteroanterior (PA) cephalograms and found out that images of landmarks near the ear rod plane will be shifted approximately 1 mm towards the contralateral side for each 10mm of shift in the horizontal position of the focal spot. Similar conclusion was also made in another study in which influence of rotational changes in head were evaluated on lateral cephalograms and were found to be between 16.1 to 44.7 per cent changes in the horizontal and angular measurements for a 14 degree rotation of the head.[31] Furthermore, Ahlqvist et al.,[32] consider 5 degrees of rotation or less to be acceptable in head positioning, as this would only result in an insignificant error (less than 1 per cent) in lateral cephalometric distance measurements.

Common Variations in Measurements

Variation in linear and angular measurements is common in the current orthodontics litarture.[12-17] Using different lateral cephalogram machines with various methods of conversion of 3D images to 2D can result in a range of findings. Damstra et al.,[25] used a mid-sagittal approach to position the bilateral structures and found no significant difference between the two and three-dimensional measurements. Oz et al.,[33] compared measurements from Planmeca PM 2002 cc Proline and NewTom 3G and concluded that both modalities yielded similar results. Pittayapat et al.,[34] also did not find 3D images to be any superior to 2D images in terms of accuracy of linear cephalometric measurements other than more accurate reproducibility with CBCT; whereas, Moshiri et al.,[17] found that out of the 9 linear measurements conventional lateral cephalograms were

only accurate for porion-orbitale (Po-Or) and anterior nasal spine-nasion (ANS-N) measurements, and that the CBCT images were accurate for all the measurements except pogonion-gonion (Pog-Go), and gonion-menton (Go-Me).

Comparison of Siorna and NewTom Lateral Cephalograms

In a thesis study conducted by Da Lee, statistically significant differences were found in percent magnification in the horizontal and vertical measurements made on lateral cephalograms taken by Sirona Orthopos XG Plus and NewTom 5G CBCT using a radiographic phantom. Even though the Ricketts cephalometric analysis on a sample of forty patients were found to be clinically comparable, the difference in magnification was concluded to impose difficulty in obtaining accurate superimposition between images produced by the two machines.[35]

Statement of the Problem

The continued use of previously published cephalometric data can only be done if CBCT images are found to be comparable to conventional 2D imaging. Furthermore, 2D lateral cephalograms taken as progress records could be compared to initial records (T1) taken with 3D imaging, which could eliminate the need for 3D cephalometric progress records.

Null-Hypothesis

Pilot Study

1. There is no perspective magnification in lateral cephalograms from Siorna Orthophos XG Plus and Dophin™ generated NewTom 5G CBCT perspective and orthogonal projections.
2. There is no difference in linear measurements of N-Ba and N-Me between Dophin™ generated NewTom 5G CBCT in orthogonal projection adjusted to 100%,101%, 102% , and 103% magnification and Sirona Orthophos XG Plus.

Main Study

There is no difference in Ricketts analysis lateral cephalometric measurements between Sirona Orthophos XG Plus and Dophin™ generated NewTom 5G Orthogonal projection at varying magnification.

Material and Methods

Phantom Construction

This study was approved by Institutional Review Board (IRB) at Loma Linda University, Loma Linda, CA. Because of the inherent difficulty in measuring landmarks on lateral cephalograms, an imaging phantom was constructed. A 15x15x15 cm 3D imaging phantom was constructed using six 2.5 cm thick styrofoam slabs arranged in parasagittal planes (Fig 1). This allowed placement of a 15x15 cm metallic plastics (alumide) gird at selected midsagittal and parasagittal planes. The grid had 0.5x0.5 cm elements and was computer generated and printed to maximize uniformity of grid cell

size. Spacers were added to the parasagittal planes closest to the midsagittal plane so that the distance between those planes would simulate the average intermolar distance (5.7 cm). Before imaging procedures, the grid could be moved to one of these three sagittal planes (left, center, right). During panorex imaging procedures, the right side parasagittal plane was always positioned closest to the x-ray sensor.

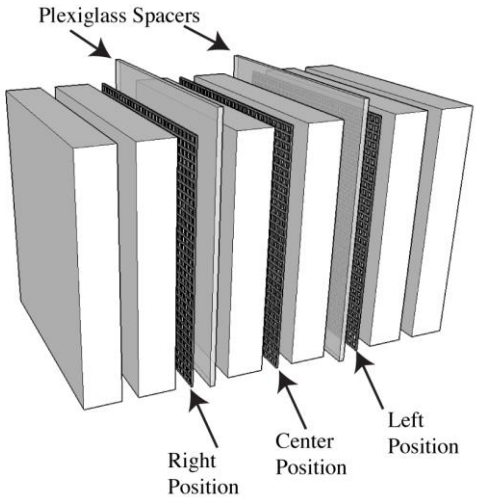

Figure 1. Exploded view of the radiographic phantom. This graph shows alumide grid in the three sagittal planes.

A custom acrylic box was fabricated to accommodate the phantom elements (Fig 2). A 3.0 cm by 0.7 cm rectangular slot was designed at the location of Nasion. Porion location was marked on the two outer styrofoam blocks. A 3.0x0.7 cm rectangular slot was cut into the acrylic box at the location of nasion.

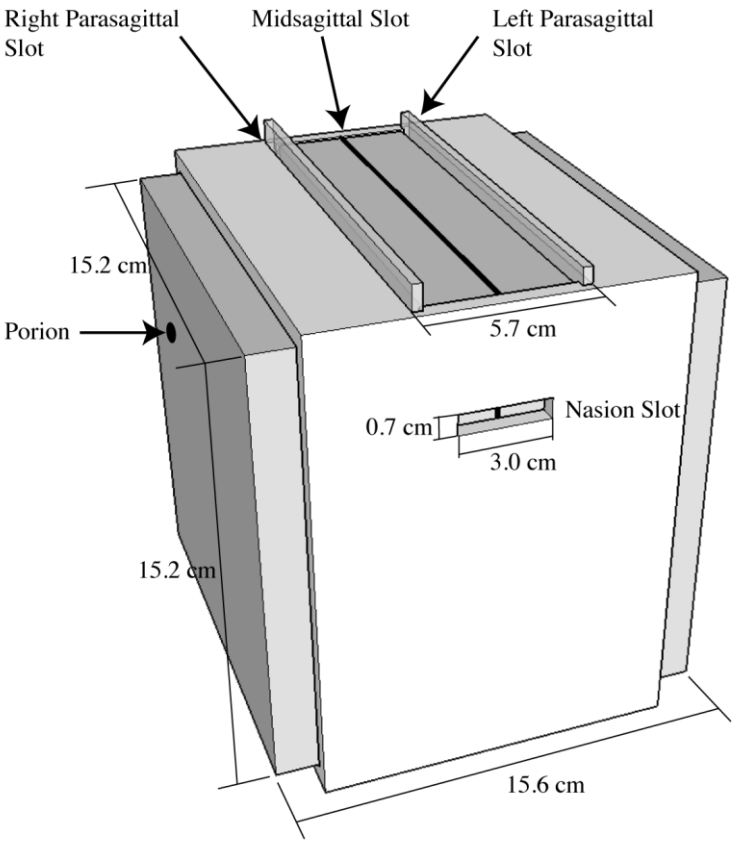

Figure 2. Radiographic phantom box. Three sagittal planes were designed for placement of aumide grid. A Nasion slot was designed to match the nose piece of the Sirona machine. The location of Porion was marked on the two outer styrofoam blocks to symmetrically position the phantom between the ear rods.

Positioning the Phantom for Panoramic X-ray

In order to eliminate inter-operator error, all panoramic images were taken by one person (Y.J.). The Acrylic box was positioned on a stand and adjusted for the ear rods to be positioned on the outer surfaces of the styrofoam blocks where Porion was marked, and the nose piece of the panorex machine was aligned with the nasion slot of the acrylic box. The light localizer of the Sirona Orthophos XG Plus (Sirona Dentral Systems Inc, NY) was used to ensure passage of the x-ray beam through the center of the phantom in both horizontal and vertical dimensions. Once the ideal position of the acrylic box was

established, the box was attached to the stand to prevent any unwanted movement. Only the grid position was changed from right to center to left.

Positioning the Phantom for CBCT Imaging

The NewTom 5G CBCT (NewTom 5G; QR srl, Verona, Italy) was equipped with two cross shaped laser guides that were used to properly position the phantom in the x-ray beam. Phantom position was adjusted so that the vertical guide passed through the midsagittal plane and the horizontal guide passed through the central axial plane. Scout images were taken to evaluate the symmetrical positioning and exposure of the phantom.

Phantom Measurements

Digital lateral cephalograms, Sirona Orthophos XG and synthesized CBCT lateral cephalograms in orthogonal and perspective projections were imported into Dolphin™ 3D (version 11.8; Dolphin Imaging & Management Solutions, Chatsworth, Calif.). The total horizontal, total vertical, mid-horizontal, and mid-vertical distances were measured in each plane using National Institute of Health (NIH) ImageJ 1.50b program (Fig 3). The aumide grid was also scanned outside of the phantom and measured using the same program. These measurements were repeated by the same person for a total of ten times at one week intervals.

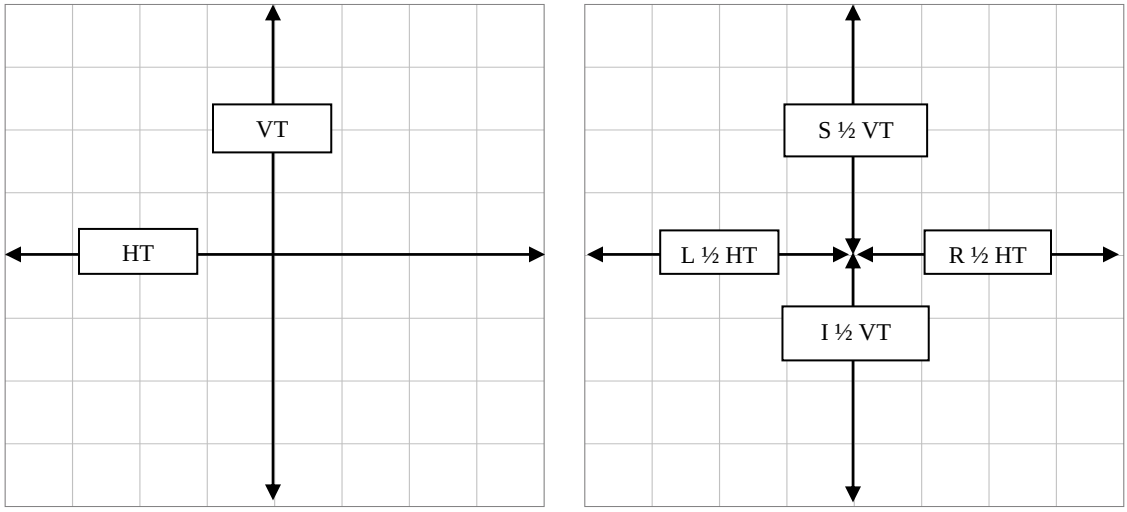

Figure 3. Phantom measurements. L ½ HT (left horizontal half), R ½ HT (right horizontal half), S ½ VT (superior vertical half), I ½ VT (inferior vertical half), HT (total horizontal), VT (total vertical).

Clinical Data Collection

This study was approved by Institutional Review Board (IRB) at Loma Linda University, Loma Linda, CA. Twenty-five lateral cephalometric radiographs were selected retrospectively from the records of patients of the Loma Linda University School of Dentistry, Graduate Orthodontic Clinic from December 1, 2015 to March 30, 2016. The radiographs must have been taken according to standard head positioning methods: 1) Sirona, using ear rods and alignment of the frontal Frankfort plane with the optical guide, 2) NewTom, using laser guides to align the sagittal and occlusal planes to the x-ray beam. Radiographs were excluded from the study if they displayed occlusal plane discrepancy (>2 mm), or missing first molars.

CBCT synthesized lateral cephalograms in the perspective and orthogonal projections with the projection center at porion were produced in Dolphin^{TM} 3D. The

resulting constructed images were then flipped horizontally to match the orientation of the Sirona lateral cephalograms (Figs 4,5). Images were traced in Dolphin^{TM} using the Ricketts analysis. Additionally, two linear measurements, Nasion to Basion (N-Ba) and Nasion to Menton (N-Me) were used to evaluate magnification on a larger scale (Table 1).

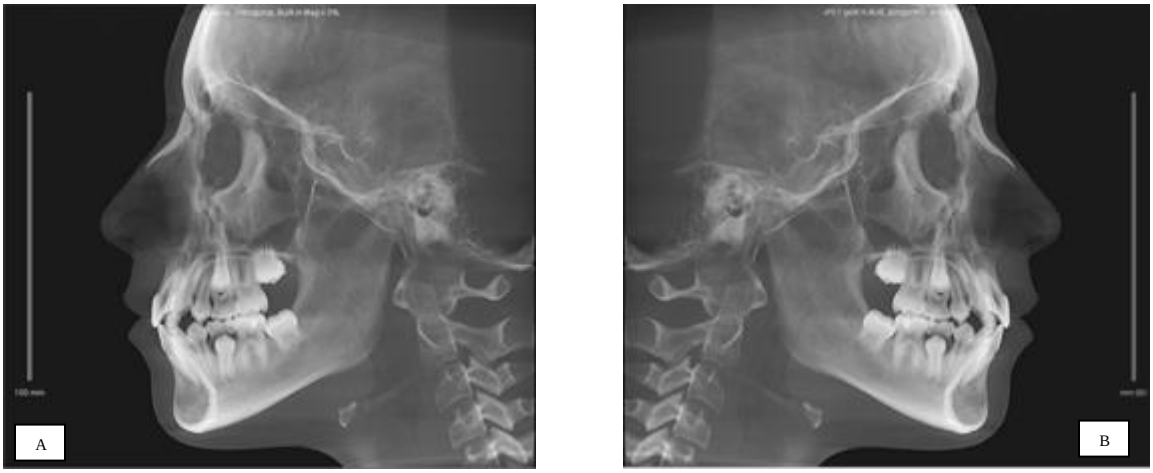

Figure 4. Construction left lateral cephalogram with x-ray beam centered on porion (A). Image A being horizontally flipped (B).

Figure 5 Sirona lateral cephalogram and Dolphin^{TM} generated CBCT cephalograms. Sirona Orhthophos lateral cephalogram (A) and mirrored images of construction left lateral cephalogram in perspective (B) and Orthotogonal projection (C).

Table 1. Angular and linear measurements.

Angular Measurements (°)	Linear Measurements (mm)
1. Cranial Deflection (N-Ba to FH)	1. Convexity (A-NPo)
2. Facial Depth (FH-NPo)	2. Cranial Length (CC-N)
3. Facial Axis (NaBa-PtGn)	3. L1 Protrusion (L1-APo)
4. Mandibular Plane (GoGn-FH)	4. Lower Lip to E-Plane
5. Interincisal Angle (U1-L1)	5. U-Incisor Protrusion (U1-APo)
6. L1 to A-Po	6. U6-PT Vertical
7. Lower Face Height (ANS-Xi-Pm)	7. Nasion to Basion (N-Ba)
8. Mandibular Arc (PmXi-XiDC)	8. Nasion to Menton (N-Me)
9. Maxillary Depth (FH-NA)	

Intraexaminer and Interexaminer Reliability

To test intraexaminer reliability, five randomly selected Sirona lateral cephalograms were digitized three times, by the same examine (Y.J) with one week intervals between digitizing sessions. Digitizing was done with Dolphin^{TM} 3D and Ricketts analysis measurements were used to evaluate repeatability. The same set of five cephalograms was digitized by another examiner to evaluate inter-examiner repeatability. The Ricketts Analysis points and planes and additional N-Me and N-Ba planes are shown in Figure 6.

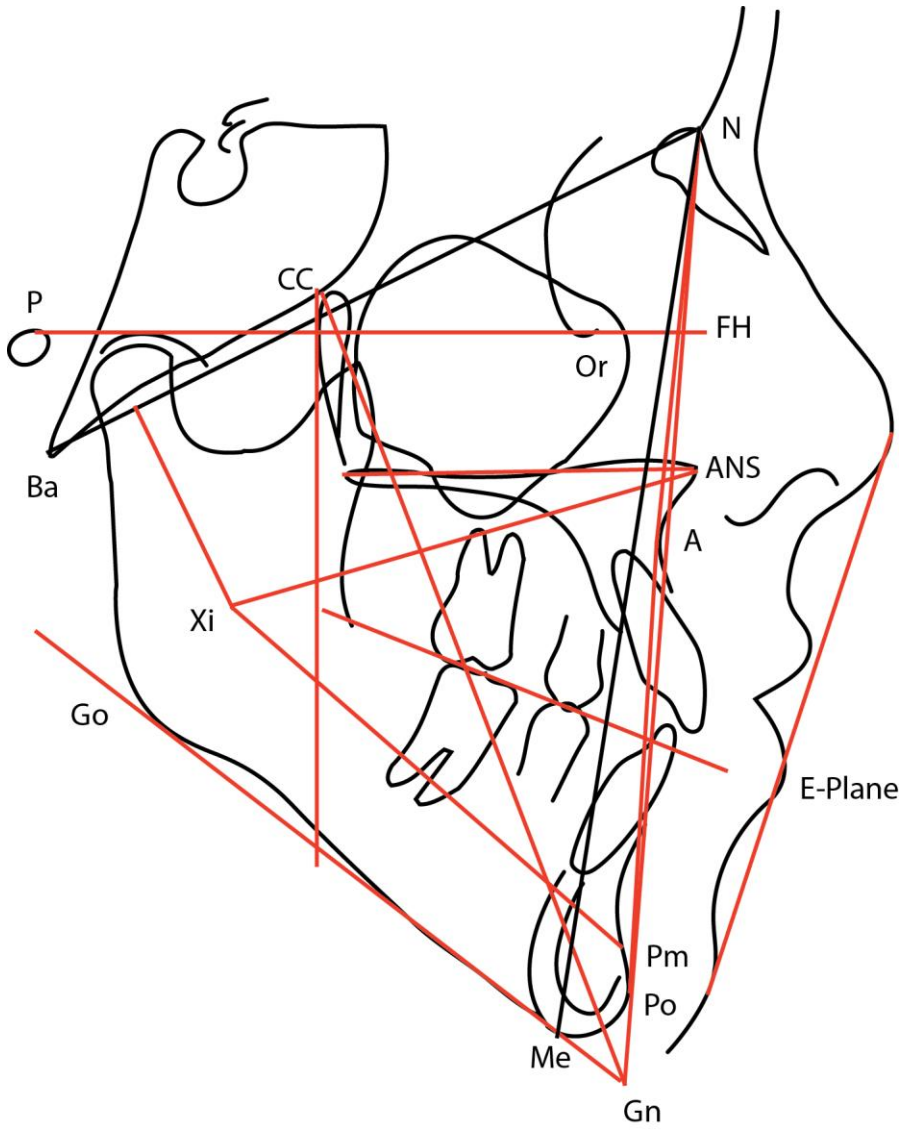

Figure 6. Landmarks and reference planes. Two additional planes, N-Ba and N-Me are also shown.

Statistical Analysis

Statistical analysis was performed using IBM SPSS 21.0 (IBM Corp., Armonk, NY, USA) at $\alpha = 0.05$. The reliability of measurements on radiographic phantom was analyzed using a correlation test. The agreement among the vertical and horizontal measurements on the metal grid, the Sirona Orthophos XG Plus digital lateral

cephalogram, the Dolphin^{TM} generated CBCT lateral cephalogram in the perspective and orthogonal projections were analyzed using the Wilcoxon signed rank test. Intraclass correlation coefficient tests were used to determine intraexaminer and interexaminer reliability. The sample size (n=25) was justified at the power of 95%, alpha value of 0.05 to determine the effect size of 1.3 when comparing the Ricketts measurement of the pre and post adjusted CBCT images (Alpha pre and Alpha post) to the non-adjusted Sirona.

The measurements between the Sirona Orthophos XG Plus digital lateral cephalograms and the adjusted CBCT lateral cephalograms in orthogonal projection were compared using one sample Wilcoxon signed rank text. Nonparametric tests were performed to adjust for measurements in which the data did not show a normal distribution.

Results

Table 2 shows the reliability of repeated measurements by a single operator. High reliability for the repeated measurements on the radiographic phantom is indicated by the high intra-class correlation values. Tables 3 and 4 show the comparison of means and standard deviation for vertical and horizontal halves measurements between the right, center and left side grid using each imaging modality as well as the measurements made on the scanned grid. The differences between the means for each modality is also shown. Slightly greater differences were detected for repeated measurements in the vertical halves. Difference in the vertical direction varied between -0.01 mm to -0.38 mm, whereas the difference in the horizontal direction varied between -0.01 mm to -0.27 mm. None of these however, reached clinical significance (0.6 mm).

Table 2. Reliability of measurements on radiographic phantom using correlation test.

Modality	Intraclass Correlation[b]	95% Confidence Interval	
		Lower Bound	Upper Bound
Grid	1.000[a]	1.000	1.000
Sirona R	1.000[a]	1.000	1.000
Sirona C	1.000[a]	1.000	1.000
Sirona L	1.000[a]	1.000	1.000
CBCT PR	1.000[a]	1.000	1.000
CBCT PC	1.000[a]	1.000	1.000
CBCT PL	1.000[a]	1.000	1.000
CBCT OR	1.000[a]	1.000	1.000
CBCT OC	1.000[a]	1.000	1.000
CBCT OL	1.000[a]	1.000	1.000

Two-way random effects model where both people effects and measures effects are random.
a. The estimator is the same, whether the interaction effect is present or not.
b. Type A intraclass correlation coefficients using an absolute agreement definition.

Table 3. Comparison of Mean ± Standard Deviation (mm) of vertical measurements using Related Samples Wilcoxon Signed Rank Test at $\alpha = 0.05$.

	S ½ VT Mean±SD (mm)	I ½ VT Mean±SD (mm)	Difference S ½ VT - I ½ VT Mean±SD (mm)	P-Value
Grid	64.20±0.14	64.12±0.17	0.08±0.23	0.497
Sirona R	64.22±0.29	64.19±0.25	0.03±0.19	0.733
Sirona C	65.28±0.19	65.66±1.05	-0.38±1.18	0.674
Sirona L	66.51±0.30	66.51±0.26	-0.01±0.47	1.000
CBCT PR	70.76±0.26	70.93±0.24	-0.17±0.21	0.036*
CBCT PC	71.00±0.31	70.65±0.22	0.35±0.39	0.028*
CBCT PL	71.06±0.33	71.05±0.27	0.02±0.39	0.767
CBCT OR	64.82±0.22	64.44±0.19	0.38±0.36	0.021*
CBCT OC	64.74±0.21	64.61±0.38	0.14±0.47	0.241
CBCT OL	64.55±0.23	64.92±0.27	-0.37±0.23	0.007*

Asymptotic significances are displayed. The significance level is $\alpha = 0.05$.
* Denotes statistical difference.

Table 4. Comparison of Mean ± Standard Deviation (mm) of horizontal measurements using Related Samples Wilcoxon Signed Rank Test at $\alpha = 0.05$.

	L ½ HT Mean±SD (mm)	R ½ HT Mean±SD (mm)	Difference L ½ HT - R ½ HT Mean±SD (mm)	P-Value
Grid	64.37±0.23	64.27±0.19	0.10±0.17	0.345
Sirona R	64.24±0.34	64.18±0.19	0.06±0.31	0.674
Sirona C	65.34±0.13	65.37±0.19	-0.03±0.22	0.612
Sirona L	66.39±0.10	66.43±0.22	-0.04±0.19	0.324
CBCT PR	70.46±0.18	70.27±0.30	0.19±0.29	0.091
CBCT PC	70.90±0.17	70.50±0.20	-0.21±0.16	0.018*
CBCT PL	70.44±0.27	70.67±0.25	-0.24±0.31	0.061
CBCT OR	64.30±0.15	64.02±0.19	0.27±0.20	0.011*
CBCT OC	64.20±012	64.28±0.16	-0.09±0.20	0.144
CBCT OL	64.52±0.24	64.53±0.23	-0.01±0.16	0.932

Asymptotic significances are displayed. The significance level is $\alpha = 0.05$.
* Denotes statistical difference

Table 5 shows the comparison of means and standard deviations for total vertical and total horizontal measurements taken from the scanned grid, Sirona Orthophos XG Plus lateral cephalogram, Dolphin™ generated CBCT lateral cephalogram in the perspective and orthogonal projections. The percent magnification between the grid and each imaging modality is also displayed. For images obtained by Sirona Orthophos XG Plus, the magnification gradually increases as grid is moved from right (closest to the sensor) to left (farthest from the sensor). Greatest magnification changes are observed

when comparing the image of scanned grid to the images from Dolphin™ generated CBCT in perspective projection. Magnification differences vary from 110.22% to 110.60% in the vertical direction and 109.60% to 109.67% in the horizontal direction. Furthermore, when images from right, center and left sides are compared, Dolphin™ generated CBCT lateral cephalogram in perspective projection produces images with only slight difference in the magnification, therefore, it does not result in a truly perspective image. Right side grid on Sirona Orthophos XG Plus and NewTom 5G CBCT orthogonal had the closest agreement to the grid for both vertical and horizontal measurements.

Table 5. Comparison of mean ± standard (mm) deviation and % magnification compared to the grid.

	Mean ± SD (mm) Right	% Mag* Right	Mean ± SD (mm) Center	% Mag* Center	Mean ± SD (mm) Left	% Mag* Left
			Total Vertical Measurements			
Grid	128.38±0.18	100	128.38±0.18	100	128.38±0.18	100
Sirona	128.20±0.32	99.87	130.69±0.26	101.80	133.03±0.25	103.63
CBCT P	141.63±0.43	110.32	141.49±0.26	110.22	142.01±0.37	110.62
CBCT O	129.30±0.13	100.72	129.36±0.23	100.77	129.56±0.27	100.63
			Total Horizontal Measurements			
Grid	128.34±0.22	100	128.34±0.22	100	128.34±0.22	100
Sirona	128.36±0.33	100.02	130.63±0.27	101.79	132.97±0.28	103.61
CBCT P	140.66±0.43	109.60	140.75±0.28	109.67	141.09±0.41	109.94
CBCT O	128±0.25	100.07	128.57±0.22	100.18	129.14±0.47	100.93

* % Magnification is calculated for each modality compared to grid.

Tables 6 and 7 summarizes the reliability test on repeated measurements by the two examiners. High intraclass correlation coefficients indicate strong intraexaminer and interexaminer reliability for the Ricketts analysis measurements.

Table 6. Intraexaminer reliability- Sirona

	Intraclass Correlation[b]	95% Confidence Interval	
		Lower Bound	Upper Bound
Single Measures	.999[a]	.999	1.000
Average Measures	1.000	1.000	1.000

a. The estimator is the same, whether the interaction effect is present or not.

b. Type A intraclass correlation coefficients using an absolute agreement definition.

Table 7. Interexaminer reliability- Sirona

	Intraclass Correlation[b]	95% Confidence Interval	
		Lower Bound	Upper Bound
Single Measures	.999[a]	.998	.999
Average Measures	.999	.999	1.000

a. The estimator is the same, whether the interaction effect is present or not.
b. Type A intraclass correlation coefficients using an absolute agreement definition.

The agreement between measurements from Sirona Orthophos XG Plus and Dolphin™ generated CBCT perspective lateral cephalograms is summarized in Tables 8 and 9. The linear and angular measurements are analyzed separately. Statistically significant differences were found between all linear measurements with the exception of lower lip to E-plane. Overall, the difference ranged from 0.20 mm to -8.36 mm and

measurements including, cranial length, U-incisor protrusion, U6-PTV, N-Ba, and N-Me reached clinical significance (0.6 mm). When comparing the angular measurements between these two modalities, statistically significant difference was only found for the facial axis (P =0.015).

Table 8. The agreement between linear measurements from Sirona Orthophos XG Plus and Dolphin™ generated CBCT perspective lateral cephalograms via One-Sample Wilcoxon Signed Rank test at $\alpha = 0.05$.

Linear Measurements	Sirona Mean ± SD (mm)	CBCT Perspective Mean ± SD (mm)	Mean of Difference ± SD (mm) [a]	P-Value
Convexity	3.42 ± 3.03	3.69 ± 3.24	-0.25±0.46	0.004*
Cranial Length	56.26 ± 2.89	60.66 ± 3.25	-4.07±1.66	<0.001*
L1 Protrusion	2.82 ± 2.17	3.20 ± 2.28	-0.38±0.44	<0.001*
Lower Lip to E-Plane	-1.07 ± 2.65	-1.33 ± 2.82	0.20±0.86	0.088
U-Incisor Protrusion	5.92 ± 2.37	6.58 ± 2.62	-0.64±0.52	<0.001*
U6-PT Vertical	18.38 ± 3.40	19.35 ± 2.64	-0.92±0.76	<0.001*
Nasion to Basion	100.51 ± 4.67	108.64 ± 4.71	-7.59±2.55	<0.001*
Nasion to Menton	104.94 ± 7.90	113.94 ± 8.35	-8.36±2.59	<0.001*

Asymptotic significances are displayed. The significance level is $\alpha = 0.05$.
a. Difference was found by subtracting CBCT measurements from Sirona.
* Denotes statistical difference.

Table 9. The agreement between angular measurements from Sirona Orthophos XG Plus and Dolphin™ generated CBCT perspective lateral cephalograms via One-Sample Wilcoxon Signed Rank test at $\alpha = 0.05$.

Angular Measurements	Sirona Mean ± SD (deg)	CBCT Perspective Mean ± SD (deg)	Mean of Difference ± SD (deg) [a]	P-Value
Cranial Deflection	29.66±1.72	29.66±2.03	-0.06±0.88	0.500
Facial Angle	89.74±2.64	89.54±2.80	0.18±0.51	0.046
Facial Axis	88.70±3.94	88.26±3.95	0.34±0.90	0.015*
Mandibular plane angle	21.34±4.82	21.40±5.17	-0.06±0.93	0.401
Interincisal angle	127.34±12.64	127.34±12.47	0.01±0.73	0.490
L1 to A-Po	24.40±5.92	24.39±5.98	0.06±1.05	0.472
Lower Face Height	43.46±4.07	43.50±4.13	-0.12±0.83	0.408
Mandibular Arc	35.96±5.33	35.95±4.87	0.06±1.81	0.484
Maxillary Depth	93.06±3.21	92.90±3.43	0.18±0.60	0.108

Asymptotic significances are displayed. The significance level is $\alpha = 0.05$.
a. Difference was found by subtracting CBCT measurements from Sirona.
* Denotes statistical difference.

Tables 10 and 11 summarize the agreement between measurements from Sirona Orthophos XG Plus and Dolphin™ generated CBCT orthogonal lateral cephalograms at 100%, 101%, 102% and 103% magnification. The linear and angular measurements are analyzed separately. At 100% of magnification, statistically significant difference was found in all linear measurements except for lower lip to E-plane. Cranial length, U6-PTV, N-Ba, and N-Me reached clinical significance (0.6 mm). The angular measurements only showed statistically significant difference in facial axis measurement (P =0.004).

Table 10. The agreement between linear measurements from Sirona Orthophos XG Plus and Dolphin™ generated CBCT orthogonal lateral cephalograms at 100%, 101%, 102%, and 103% magnification via One-Sample Wilcoxon Signed Rank test at $\alpha = 0.05$.

Linear Measurements	Sirona Mean ± SD (mm)	Difference Sirona – CBCT 100%		Difference Sirona – CBCT 101%		Difference Sirona – CBCT 102%		Difference Sirona – CBCT 103%	
		Mean ± SD (mm)	P-Value	Mean ± SD (mm)	P-Value	Mean ± SD (mm)	P-Value	Mean ± SD (mm)	P-Value
Convexity	3.42 ± 3.03	0.2±0.32	0.002*	0.2±0.30	0.006*	0.1±0.30	0.013*	0.1±0.29	0.046*
Cranial Length	56.26 ± 2.89	1.2±1.15	<0.001*	0.6±1.13	0.012*	0.1±1.12	0.678	-0.4±1.13	0.113
L1 Protrusion	2.82 ± 2.17	0.2±0.35	0.008*	0.2±0.34	0.009*	0.1±0.34	0.019*	0.1±0.34	0.039*
Lower Lip to E-Plane	-1.07 ± 2.65	0.1±0.86	0.544	0.1±0.85	0.435	0.1±0.86	0.399	0.2±0.86	0.360
U-Incisor Protrusion	5.92 ± 2.37	0.1±0.33	0.027*	0.1±0.34	0.083	0.0±0.33	0.250	-0.1±0.35	0.870
U6-PT Vertical	18.38 ± 3.40	0.7±0.49	<0.001*	0.6±0.48	<0.001*	0.4±0.46	<0.001*	0.2±0.44	0.024*
Nasion to Basion	100.51 ± 4.67	1.3±0.84	<0.001*	0.3±0.73	0.006*	-0.6±0.75	0.007*	-1.5±0.83	<0.001*
Nasion to Menton	104.94 ± 7.90	1.1±0.86	<0.001*	0.1±0.81	0.875	-0.9±0.84	0.001*	-1.9±0.96	<0.001*

Asymptotic significances are displayed. The significance level is 0.05.
a. Difference was found by subtracting CBCT measurements from Sirona.
* Denotes statistical difference.

Table 11. The agreement between angular measurements from Sirona Orthophos XG Plus and Dolphin™ generated CBCT orthogonal lateral cephalograms at 100%, 101%, 102%, and 103% magnification via One-Sample Wilcoxon Signed Rank test at $\alpha = 0.05$.

Angular Measurements	Sirona Mean ± SD (deg)	Difference Sirona – CBCT 100%		Difference Sirona – CBCT 101%		Difference Sirona – CBCT 102%		Difference Sirona – CBCT 103%	
		Mean ± SD (deg)	P-Value	Mean ± SD (deg)	P-Value	Mean ± SD (deg)	P-Value	Mean ± SD (deg)	P-Value
Cranial Deflection	29.66±1.72	-0.3±0.92	0.411	-0.3±0.92	0.411	-0.3±0.92	0.411	-0.3±0.92	0.411
Facial Angle	89.74±2.64	0.1±0.49	0.277	0.1±0.48	0.310	0.1±0.48	0.310	0.1±0.48	0.310
Facial Axis	88.70±3.94	0.5±0.91	0.004*	0.5±0.91	0.004*	0.5±0.90	0.004*	0.5±0.90	0.004*
Mandibular plane angle	21.34±4.82	-0.2±0.89	0.182	-0.2±0.89	0.182	-0.2±0.89	0.189	-0.2±0.88	0.189
Interincisal angle	127.34±12.64	-0.1±0.51	0.253	-0.1±0.51	0.253	-0.1±0.51	0.253	-0.1±0.51	0.308
L1 to A-Po	24.40±5.92	-0.3±1.12	0.319	-0.3±1.12	0.319	-0.3±1.12	0.319	-0.3±1.12	0.319
Lower Face Height	43.46±4.07	0.1±0.81	0.253	0.1±0.81	0.253	0.1±0.81	0.253	0.1±0.81	0.253
Mandibular Arc	35.96±5.33	0.1±1.80	0.658	0.1±1.80	0.657	0.1±1.80	0.647	0.1±1.80	0.647
Maxillary Depth	93.06±3.21	0.2±0.46	0.025*	0.2±0.45	0.025*	0.2±0.45	0.025*	0.2±0.45	0.025*

Asymptotic significances are displayed. The significance level is 0.05.
a. Difference was found by subtracting CBCT measurements from Sirona.
* Denotes statistical difference.

At 101% magnification, statistically significant differences were found in all linear measurements except for lower lip to E-plane, upper incisor protrusion and Nasion to Menton. Only two of them, including cranial length and U6-PTV reached clinical significance (0.6 mm). When CBCT orthogonal at 102% and 103% magnification were compared to Sirona, statistically significant differences were found in all linear measurements except for cranial length, lower lip to E-plane and upper incisor protrusion. Clinically significant differences were only found in N-Ba and N-Me measurements. Statistical differences in two angular measurements, facial axis (P =0.004), maxillary depth measurements (P =0.025) were found in all adjusted CBCT orthogonal cephalograms.

Comparison between Sirona Orthophos XG Plus and NewTom 5G CBCT orthogonal at various magnification based on Nasion to Basion and Nasion to Menton measurements indicated statistically significant differences between the two entities at all magnifications except the orthogonal projection at 101% magnification (Table 12). When Sirona and CBCT orthogonal lateral cephalograms are compare by combining N-Ba and N-Me measurements, CBCT orthogonal at 101% magnification has the mean difference closest to zero (Fig 7).

Table 12. Comparison of Sirona Orthophos XG Plus and Dolphin™ generated CBCT orthogonal at various adjusted magnification based on two linear measurements of Nasion to Basion and Nasion to Menton.

NewTom 5G CBCT Orthogonal %	Nasion to Basion Mean ± SD (mm) [a]	P-Value	Nasion to Menton Mean ± SD (mm)	P-Value
100%	1.3±0.84	<0.001*	1.1±0.86	<0.001*
101%	0.3±0.73	0.006*	0.1±0.81	0.875
102%	-0.6±0.75	0.007*	-0.9±0.84	0.001*
103%	-1.5±0.83	<0.001*	-1.9±0.96	<0.001*

a. The difference was calculated by subtracting CBCT measurements from Sirona.
***** Denotes statistical difference.

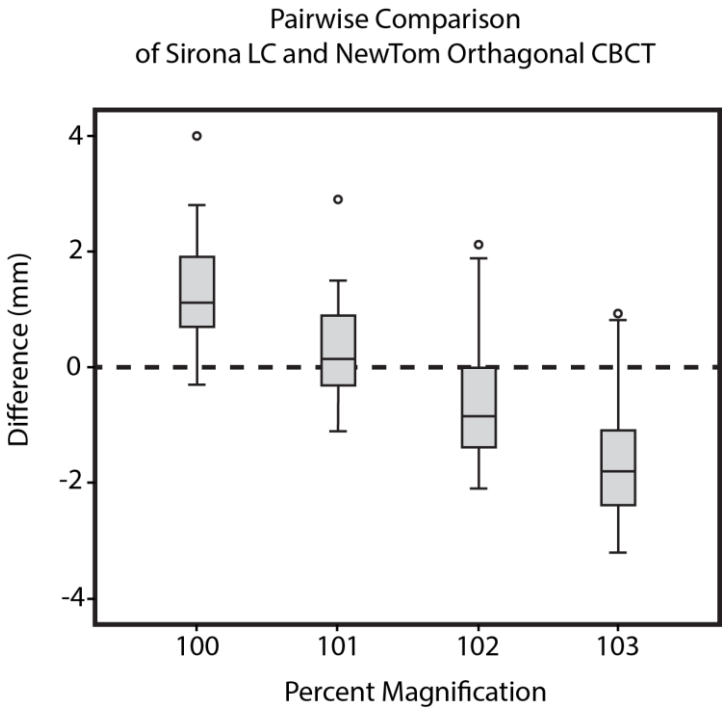

Figure 7. Pairwise comparison of Sirona LC and Dolphin™ generated CBCT in orthogonal projection. Adjusted magnifications are compared based on two linear measurements of Nasion to Basion and Nasion to Menton.

Discussion

Cone-beam computed tomography (CBCT) is becoming established as an alternative tool and, in many aspects, superior radiographic technique to conventional radiography in orthodontics.[3] However, cephalometric analysis is still an important tool for treatment planning because 3-dimentional analyses are still not established. The purpose of this study was to determine whether Ricketts cephalometric analysis performed on Dolphin™ generated CBCT synthesized lateral cephalograms could provide the same measurements as of those on the Sirona Orthophos XG Plus digital.

To eliminate patient positioning as well as landmark identification errors described by Lee et al.,[30] a radiographic phantom was custom-made to represent an

average adult skull. The radiographic phantom was then used to analyze the possible magnification differences as well as single plane and multiplane perspective distortion between lateral cephalograms obtained from Sirona Orthophos XG Plus and Dolphin™ generated CBCT in perspective and orthogonal projections. One would expect that the measurements of the grid to be the same as the measurements obtained from CBCT in orthogonal view since the orthogonal projection by definition creates 1:1 images, regardless of the object to receptor distance. We also expected to get images that would magnify gradually as the grid was moved farther away from the receptor (multiplane perspective distortion) in the Sirona and Dolphin™ generated CBCT with perspective projection.

The analysis of the difference among the vertical halves and horizontal halves was the method used in this study to evaluate the presence of single and multiplane perspective distortion. If there was a perspective distortion, we would expect to see differences between these measurements. The differences among the vertical halves and horizontal halves showed statistically significant differences for Dolphin™ generated images in CBCT perspective center grid and CBCT orthogonal right grid in the vertical direction, and CBCT perspective left, right and CBCT orthogonal right and left in the horizontal direction (Tables 3 and 4). The calculated difference ranged as low as -0.01±0.16 mm to as high as 0.38±0.36 mm, with the greatest difference being in the vertical direction. These differences, although statistically significant, did not reach clinical significance (0.6 mm).[2]

Furthermore, for imaging techniques that use non-parallel beam (Sirona and Dolphin™ CBCT perspective), if the x-ray beam passed through porion, we expected to

see single plane perspective distortion in the areas away from porion. Our findings based on the measurements of the vertical and horizontal halves, however, rejects this analogy. This may suggest that the algorithm used in these two imaging modalities corrects for single plane perspective distortion.

When comparing actual grid measurements to each of the three imaging modalities (Table 5), Sirona with the alumide grid on the right side was found to have the best agreement to the grid followed by Dolphin^{TM} generated CBCT lateral cephalograms in orthogonal projection with the alimude grid on the right side. In this case Sirona presented a multiplane perspective distortion, meaning that measurements enlarged by roughly 1% as the alumide grid was moved farther away from the sensor. As expected, no multiplane perspective distortion was observed in orthogonal projection. When comparing the images from Sirona to those of Dolphin^{TM} generated CBCT in orthogonal projection, images of the right side grid were least magnified and these measurements were closest to the actual grid measurements. This finding suggests that in order to get the most accurate measurements, in cases with bilateral structures, the structures on the side closest to the film should be selected, as these would represent the real measurements more closely. Unlike the other two modalities, Dolphin^{TM} generated CBCT lateral cephalograms in perspective projection produced images with the highest magnification (~10%) when compared to the grid. Furthermore, the images from Dolphin^{TM} generated CBCT in perspective projection did not represent multiplane perspective distortion, as measurements were enlarged in three different planes by the same magnification (~10%). This suggests that the algorithm used by Dolphin^{TM} 3D to

synthesize images in perspective projection uses a magnification similar to that of the analog films without replicating the perspective distortion.

For the patient group used in this study, operator error was controlled at multiple levels. All images were taken by the same person. In order to reduce projection error described in literature,[30,32] patients were positioned in the Sirona Orthophos XG Plus and NewTom 5G machine according to the standard head positioning methods. Patient positioning was further evaluated in the NewTom 5G machine via scout images. To reduce landmark identification error, exclusion criteria were also used to eliminate cases with occlusal plane discrepancy of >2 mm, and missing first molars. NewTom 5G 3D volumes were adjusted to produce images in the same orientation as that of Sirona Orthophos XG Plus. Images from each patient were also traced at the same setting by the same person. The analysis of error (correlation coefficient, Tables 6 and 7) showed high correlation of the repeated measures, meaning that there was a high agreement among the two examiners as well as within the measurements made by one examiner. Lastly, because the majority of linear measurements in Ricketts analysis were over short distances and would have made them more sensitive to magnitude of differences between measurements, two additional linear measurements of N-Ba and N-Me were included in this study to allow for a greater standard error.

As expected, the statistical results of one-sample Wilcoxon signed rank test showed significant difference in linear measurements, whereas angular measurements were least affected by changes in imaging modality and magnification. Similar to the results in Da Lee's study no significant difference was found in reproducibility of the measurement for lower lip to E-plane.[35] Statistically significant differences detected in

facial axis, the angle between nasion-basion plane and foramen rotundum-gnathion, is justified based on the difficulty in identifying the landmarks compromising these angular measurements. Difficulty in locating basion has been reported in previous studies.[20-21] Locating basion has been found to have a mean coefficient of variation as large as 2.60 mm. The landmark Ba was also found to have the largest regression coefficient estimate (1.42 mm).[21] These findings indicates that identification of Ba has a statistically and clinically greater error compared with other landmarks.

The low agreement that was found between Sirona Orthophos XG Plus and Dolphin ™ generated CBCT lateral cephalograms in perspective projection as a result of the phantom study was further confirmed in our patient sample (Tables 8 and 9). Similar to Da Lee's observation, linear measurements in Dolphin ™ generated CBCT lateral cephalograms were overestimated.[35] Because of poor correlation between these two techniques, no further adjustments were made on perspective projection images.

The result of the pairwise comparison test, based on combined effect of N-Ba and N-Me (Fig 7) indicates that Dolphin™ generated CBCT lateral cephalograms in orthogonal projection adjusted to 101% magnification has the closest agreement to Sirona Orthophos XG Plus. At the 101% magnification the difference of means is closest to zero (0.2±0.77 mm). Similarly, the difference of means for Ricketts analysis measurements were found to be closest to zero at 101% magnification (Tables 10 and 11). Only two of the measurements, cranial length and U6-PTV reached clinical significance (0.6 mm). The difference of means for these measurements were 0.6±1.13 mm and 0.6±1.48 mm respectively. Foramen rotundum is a common landmark used in both of these measurements. This is a bilateral structure, and difficulty in its identification may have

contributed to the statistically significant differences noted in cranial length and U6-PTV measurements.

Conclusions

1. Perspective distortion was not detected in single sagittal plane images obtained from Sirona Orthophos XG Plus and constructed images from NewTom 5G CBCT.
2. Perspective distortion is present in Sirona Orthophos XG Plus only as the object is moved away from the radiographic sensor.
3. NewTom 5G CBCT in perspective projection results in images that are magnified with the same ratio in all planes, therefore it does not produce truly perspective images.
4. Lateral cephalograms obtained from NewTom 5G CBCT in orthogonal projection at 101% magnification closely resembles lateral cephalograms taken by Sirona Orthophos XG Plus.

CHAPTER THREE

EXTENDED DISCUSSION

Study Limitations and Future Study Directions

The limitations of this study should be considered in order to further interpret its results. Landmark identification plays a major role in accuracy of the collected data; in this study however, absolute measurements between the modalities were made and variability of landmark identification was only assessed for five randomly selected Sirona lateral cephalograms. The identification error and systematic differences in landmark position should be taken into account when conventional digital cephalograms and CBCT derived cephalograms are being compared for future ability to superimpose

In this study measurements made on Dolphin^{TM} generated CBCT lateral cephalograms were compared to Sirona digital lateral cephalograms and not to those of conventional analog. Since most of the growth studies, as well as, the cephalometric norms in the past have been done on analog images, a future study can compare CBCT image to analog images to find an algorithm to convert the norms established by previous data.

In retrospective, since Dolphin^{TM} generated CBCT in orthogonal projection produces images with the least amount of distortion in all sagittal planes, it is more reasonable to not alter these images and instead make magnification correction to Sirona images for future studies.

An interesting future study could also evaluate the accuracy of superimposition of lateral cephalograms obtained from Sirona Orthophos XG Plus on Dolphin^{TM} generated NewTom 5G CBCT images in orthogonal projection adjusted for 101% magnification.

REFERENCES

1. Broadbent BH. A new x-ray technique and its application to orthodontia. Angle Orthod 1931;1:45–66.

2. Baumrind, S. and Frantz, T.C. The reliability of head film measurements. 1. Landmark identification. Am J Orthod. 1971; 60: 111–127.

3. Mozzo P, Procacci C, Tacconi A, Martini PT, Andreis IA. A new volumetric CT machine for dental imaging based on the cone-beam technique: preliminary results. Eur Radiol 1998;8:1558-64.

4. Honda, K., Larheim, T.A., Matsumoto, K., and Iwai, K. Osseous abnormalities of the mandibular condyle: diagnostic reliability of cone beam computed tomography compared with helical computed tomography based on an autopsy material. Dentomaxillofac Radiol. 2006; 35: 152–157.

5. Tsilakis, K., Syriopoulos, K., and Stamatakis, H.C. Radiographic examination of the temporomandibular joint using cone beam computed tomography. Dentomaxillofac Radiol. 2004; 33: 196–201.

6. Nakajima, A., Sameshima, G.T., Arai, Y., Homme, Y., Shimizu, N., and Dougherty, H. Two- and three-dimensional orthodontic imaging using limited cone beam-computed tomography. Angle Orthod. 2005; 75: 895–903.

7. Maki, K., Inou, N., Takanishi, A., and Miller, A.J. Computer-assisted simulations in orthodontic diagnosis and the application of a new cone beam x-ray computed tomography. Orthod Craniofac Res. 2003; 6: 95–101.

8. Swennen, G.R.J. and Schutyser, F. Three-dimensional cephalometry: spiral multi-slice vs cone-beam computed tomography. Am J Orthod Dentofacial Orthop. 2006; 130: 410–416.

9. Ludlow, J.B., Davies-Ludlow, L.E., Brooks, S.L., and Howeerton, W.B. Dosimetry of 3 CBCT devices for oral and maxillofacial radiology: CBMercuray, NewTom 3G and i-CAT. Dentomaxillofac Radiol. 2006; 35: 219–226.

10. Ngan DC, Kharbanda OP, Geenty JP, Darendeliler MA. Comparison of radiation levels from computed tomography and conventional dental radiographs. Aust Orthod J 2003;19:67–75.

11. Faubion B.H. Treatment analysis and diagnosis: A review of the literature. Am J Orthod Dentofacial Orthop. 1966; 52: 103-125.

12. Kumar V, Ludlow JB, Mol A, Cevidanes L. Comparison of conventional and cone beam CT synthesized cephalograms. Dentomaxillofac Radiol 2007;36:263-9.

13. Kumar V, Ludlow J, Cevidanes LH, Mol A. In vivo comparison of conventional and cone beam CT synthesized cephalograms. Angle Orthod 2008;78:873-9.

14. Lamichane M, Anderson NK, Rigali PH, Seldin EB, Will LA. Accuracy of reconstructed images from cone-beam computed tomography scans. Am J Orthod Dentofacial Orthop 2009;136:156-7.

15. Park CS, Park JK, Kim H, Han SS, Jeong HG, Park H. Comparison of conventional lateral cephalograms with corresponding CBCT radiographs. Imaging Sci Dent 2012;42:201-5.

16. Hilgers ML, Scarfe WC, Scheetz JP, Farman AG. Accuracy of linear temporomandibular joint measurements with cone beam computed tomography and digital cephalometric radiography. Am J Orthod Dentofacial Orthop 2005;128:803-11.

17. Moshiri M, Scarfe WC, Hilgers ML, Scheetz JP, Silveira AM, Farman AG. Accuracy of linear measurements from imaging plate and lateral cephalometric images derived from cone-beam computed tomography. Am J Orthod Dentofacial Orthop 2007;132:550-60.

18. Gribel B, Gribel MN, Manzi FR, Brooks SL, McNamara JA. From 2D to 3D: an algorithm to derive normal values for 3-dimensional computerized assessment. Angle Orthod 2011;81:3-10.

19. Lagravère MO, Low C, Flores-Mir C, Chung R, Carey JP, Heo G, Major PW. Intraexaminer and interexaminer reliabilities of landmark identification on digitized lateral cephalograms and formatted 3-dimensional cone-beam computerized tomography images. Am J Orthod Dentofacial Orthop 2010;137:598-604.

20. Chien PC, Parks ET, Eraso F, Hartsfield JK, Roberts WE, Ofner S. Comparison of reliability in anatomical landmark identification using two-dimensional digital cephalometrics and three-dimensional cone beam computed tomography in vivo. Dentomaxillofac Radiol 2009;38:262-73.

21. Chang ZC, Hu FC, Lai E, Yao CC, Chen MH, Chen YJ. Landmark identification errors on cone-beam computed tomography-derived cephalograms and conventional digital cephalograms. Am J Orthod Dentofacial Orthop 2011;289-297.

22. Delamare EL, Liedtke GS, Vizzotto MB, Silveira HL, Ribeiro JL, Silveira HE. Influence of a programme of professional calibration in the variability of landmark identification using cone beam computed tomography-synthesized and conventional radiographic cephalograms. Dentomaxillofac Radiol 2010;39:414-23.

23. Yu Sh, Nahm Ds, Baek Sh. Reliability of landmark identification on monitor-displayed lateral cephalometric images Am J Orthod Dentofacial Orthop 2007; 133: 790-796.

24. Cattaneo PM, Bloch CB, Calmar D, Hjortshoj M, Melsen B. Comparison between conventional and cone-beam computed tomography-generated cephalograms. Am J Orthod Dentofacial Orthop 2008;134:798–802.

25. Damstra J, Fourie Z, Ren Y. Comparison between two-dimensional and midsagittal three-dimensional cephalometric measurements of dry human skulls. Br J Oral Maxillofac Surg 2011;49:392-5.

26. Proffit WR, Fields HW, Jr, Sarver DM. Contemporary orthodontics. 4th ed. St. Louis: Mosby; 2007. pp. 201–202.

27. Richardson, A. A comparison of traditional and computerized methods of cephalometric analysis. Eur J Orthod. 1981; 3: 15–20.

28. Rakosi, T. An atlas of cephalometric radiology. Wolfe Medical Publications, London, United Kingdom; 1982.

29. Waitzman AA, Posnick JC, Armstrong DC, Pron GE. Craniofacial skeletal measurements based on computed tomography: Part 1. Accuracy and reproducibility. Cleft Palate Craniofac J 1992;29:112–117.

30. Lee KH, Hwang HS, Curry SR, Boyd L, Norris K, Baumrind S. Effect of cephalometer misalignment on calculations of facial asymmetry. Am J Orthod Dentofacial Orthop 2007;132:15-27.

31. Trokova B, Major P, Prasad N, Nebbe B. Cephalometric landmarks identification and reproducibility: A Meta analysis. Am J Orthod Dentofac Orthop 1997;112:165-70.

32. Ahlqvist J, Eliasson S, Welander U 1986 The effect of projection errors on cephalometric length measurements. European Journal of Orthodontics 1986; 8: 141–148.

33. Oz U, Orhan K, Abe N. Comparison of linear and angular measurements using two-dimensional conventional methods and three-dimensional cone beam CT images reconstructed from a volumetric rendering program in vivo. Dentomaxillofac Radiol 2011;40:492-500.

34. Pittayapat P, Bornstein MM, Imada TS, Coucke W, Lambrichts I, Jacobs R. Accuracy of linear measurements using three imaging modalities: two lateral cephalograms and one 3D model from CBCT data. Eur J Orthod 2015;37:202-8.

35. Lee Da. Comparison of digital and CBCT synthesized lateral cephalograms. A master thesis. Loma Linda University School of Dentistry 2013; 1-45.

APPENDIX A

PHANTOM CROSS MEASUREMENTS (MM)

Modality	HT	L 1/2 HT	R 1/2 HT	VT	S 1/2 VT	I 1/2 VT	UL-LR	UR-LL
Grid (1)	128.844	64.422	64.422	128.592	63.919	64.171	181.858	181.315
Grid (2)	128.001	64	64	128.25	64	64	180.666	181.196
Grid (3)	128.208	64.229	64.231	128.459	64.229	64.23	181.668	181.846
Grid (4)	128.459	64.23	64.231	127.957	64.229	64.229	181.67	181.315
Grid (5)	128.208	64.728	64.728	128.208	64.482	63.989	181.668	181.138
Grid (6)	128.157	64.779	64.329	128.459	64.23	63.679	181.491	181.315
Grid (7)	128.459	64.229	64.229	128.459	64.229	64.231	181.568	181.137
Grid (8)	128.459	64.48	64.078	128.461	64.231	64.229	181.668	181.137
Grid (9)	128.357	64.229	64.23	128.459	64.229	64.229	181.446	181.128
Grid (10)	128.208	64.378	64.229	128.459	64.23	64.229	180.96	181. 492
Sirona R (1)	128.23	64.231	64.231	127.997	64.231	64.231	181.443	181.304
Sirona R (2)	127.941	63.933	63.976	127.845	64.063	63.803	181.045	180.892
Sirona R (3)	127.807	63.969	63.969	127.808	64.035	63.969	181.086	180.839
Sirona R (4)	128.14	64.157	63.983	127.88	63.724	64.027	181.081	181.003
Sirona R (5)	128.162	63.843	64.233	128.205	63.973	63.973	181.25	181.003
Sirona R (6)	128.796	64.66	64.398	128.796	64.398	64.372	181.96	181.59
Sirona R (7)	128.796	64.912	64.136	128.403	64.398	64.66	182.216	182.13
Sirona R (8)	128.534	64.398	64.136	128.534	64.66	64.398	181.962	181.778
Sirona R (9)	128.534	64.396	64.6	128.513	64.66	64.398	181.961	181.319
Sirona R (10)	128.646	63.902	64.123	128.065	64.062	64.062	181.496	181.828

Phantom Cross Measurements (Mm) *Continued*.

Modality	HT	L 1/2 HT	R 1/2 HT	VT	S 1/2 VT	I 1/2 VT	UL-LR	UR-LL
Sirona C (1)	130.686	65.365	65.278	130.643	65.191	65.365	184.897	184.81
Sirona C (2)	130.730	65.365	65.365	130.730	65.300	65.430	184.974	184.800
Sirona C (3)	130.389	65.195	65.324	130.129	64.935	68.745	184.278	184.429
Sirona C (4)	131.054	65.331	65.331	131.054	65.201	65.723	185.494	185.339
Sirona C (5)	130.903	65.452	65.452	130.642	65.234	65.234	184.882	184.695
Sirona C (6)	130.469	65.104	65.625	130.729	65.365	65.104	184.514	184.327
Sirona C (7)	130.809	65.274	65.536	131.071	65.535	65.535	185.179	185.178
Sirona C (8)	130.729	65.365	65.104	130.469	65.625	65.104	184.514	184.695
Sirona C (9)	130.469	65.625	65.644	130.729	65.104	65.325	185.251	185.064
Sirona C (10)	130.052	65.285	65.026	130.657	65.285	65.026	184.655	184.305
Sirona L (1)	132.297	66.106	66.117	132.449	66.149	66.192	188.971	188.859
Sirona L (2)	133.008	66.406	66.406	133.16	66.406	66.667	188.395	188.378
Sirona L (3)	132.943	66.406	66.667	132.943	66.71	66.406	188.426	188.286
Sirona L (4)	133.16	66.45	66.406	133.138	66.016	66.927	188.334	188.071
Sirona L (5)	133.319	66.507	66.681	133.015	66.985	66.203	188.358	188.542
Sirona L (6)	132.981	66.406	66.406	133.333	66.667	66.667	188.563	188.93
Sirona L (7)	132.812	66.406	66.146	133.073	66.406	66.927	188.195	188.378
Sirona L (8)	133.073	66.406	66.667	133.073	66.406	66.406	188.38	188.194
Sirona L (9)	133.333	66.406	66.667	133.334	66.406	66.406	188.563	188.378
Sirona L (10)	132.812	66.406	66.146	132.812	66.927	66.346	188.563	188.93

Phantom Cross Measurements (Mm) *Continued*.

Modality	HT	L 1/2 HT	R 1/2 HT	VT	S 1/2 VT	I 1/2 VT	UL-LR	UR-LL
CBCT PR (1)	141.494	70.747	70.686	142.478	71.288	71.214	200.521	201.14
CBCT PR (2)	140.391	70.416	69.976	141.565	70.562	71.149	199.338	200.152
CBCT PR (3)	140.35	70.175	70.175	140.984	70.468	70.809	199.106	199.693
CBCT PR (4)	141.275	70.539	70.932	141.716	70.981	71.225	199.723	200.348
CBCT PR (5)	140.989	70.666	70.274	142.214	70.764	71.156	199.666	200.187
CBCT PR (6)	140.469	70.381	70.381	141.642	70.968	70.981	199.483	199.899
CBCT PR (7)	140.351	70.468	69.983	141.228	70.453	70.468	199.143	199.315
CBCT PR (8)	140.556	70.571	69.985	141.728	70.864	70.864	199.398	199.778
CBCT PR (9)	140.643	70.468	70.175	141.228	70.76	70.76	199.106	199.521
CBCT PR (10)	140.058	70.175	70.175	141.521	70.468	70.689	199.279	199.521
CBCT PC (1)	140.834	70.257	70.774	141.943	70.971	70.971	199.848	200.166
CBCT PC (2)	140.412	70.206	70.206	141.592	71.091	70.796	199.442	199.517
CBCT PC (3)	141.037	70.518	70.815	141.629	71.704	70.822	200.207	200.298
CBCT PC (4)	141.124	70.414	70.71	141.42	71.006	70.71	199.999	200.839
CBCT PC (5)	141.003	70.501	70.501	141.298	71.386	70.206	199.41	200.037
CBCT PC (6)	140.708	70.206	70.501	141.593	70.796	70.796	199.617	200.039
CBCT PC (7)	140.294	70.059	70.294	141.176	70.882	70.394	199.613	199.886
CBCT PC (8)	141.003	70.501	70.501	141.593	70.886	70.501	199.825	200.039
CBCT PC (9)	140.501	70.103	70.398	141.679	70.692	70.692	198.906	199.952
CBCT PC (10)	140.588	70.148	70.294	140.982	70.588	70.588	198.822	199.867

Phantom Cross Measurements (Mm) *Continued*.

Modality	HT	L 1/2 HT	R 1/2 HT	VT	S 1/2 VT	I 1/2 VT	UL-LR	UR-LL
CBCT PL (1)	141.204	70.456	70.968	142.156	71.115	70.968	200.661	200.52
CBCT PL (2)	141.056	70.088	70.674	142.229	70.968	71.261	200.937	200.52
CBCT PL (3)	140.546	69.981	70.76	142.154	71.444	71.296	201.082	200.244
CBCT PL (4)	141.575	70.678	70.678	142.232	71.116	71.554	200.684	200.837
CBCT PL (5)	141.886	70.833	71.053	142.325	71.053	71.211	200.971	201.277
CBCT PL (6)	140.643	70.468	70.76	141.52	71.637	70.76	200.142	200.14
CBCT PL (7)	141.228	70.468	70.468	142.398	70.76	70.637	200.558	200.761
CBCT PL (8)	140.936	70.76	70.468	142.105	71.345	71.053	200.141	200.554
CBCT PL (9)	141.228	70.468	70.76	141.813	70.468	71.003	200.555	200.554
CBCT PL (10)	140.611	70.16	70.16	141.194	70.742	70.742	199.885	199.266
CBCT OR (1)	128.364	64.244	64.272	129.457	64.729	64.618	182.336	182.376
CBCT OR (2)	128.319	64.436	64.159	129.204	65.044	64.159	182.566	182.878
CBCT OR (3)	128.146	64.345	64.054	129.105	64.679	64.407	181.919	181.889
CBCT OR (4)	128.469	64.566	63.903	129.353	65.229	64.124	182.31	181.995
CBCT OR (5)	128.477	64.238	63.797	129.139	64.68	64.238	182.162	181.695
CBCT OR (6)	128.318	64.159	63.938	129.424	64.823	64.602	182.252	182.098
CBCT OR (7)	129.047	64.523	64.302	129.233	64.967	64.445	182.97	182.814
CBCT OR (8)	128.54	64.159	63.938	129.204	64.823	64.602	182.409	182.254
CBCT OR (9)	128.54	64.159	64.159	129.425	64.823	64.602	182.252	182.41
CBCT OR (10)	128.097	64.159	63.717	129.425	64.381	64.602	182.566	182.41

Phantom Cross Measurements (Mm) *Continued*.

Modality	HT	L 1/2 HT	R 1/2 HT	VT	S 1/2 VT	I 1/2 VT	UL-LR	UR-LL
CBCT OC (1)	128.742	64.371	64.201	129.338	64.67	64.669	182.389	182.714
CBCT OC (2)	128.281	64.027	64.027	129.412	64.253	65.058	182.037	182.095
CBCT OC (3)	128.63	64.213	64.213	129.243	65.031	64.008	181.91	182.492
CBCT OC (4)	128.425	64.213	64.417	129.244	64.622	64.417	182.055	182.492
CBCT OC (5)	128.747	64.271	64.271	129.809	64.887	65.298	182.368	182.953
CBCT OC (6)	128.291	64.083	64.334	129.068	64.56	64.108	181.646	181.969
CBCT OC (7)	128.217	64.108	64.108	129.12	64.786	64.408	181.646	181.808
CBCT OC (8)	128.798	64.046	64.626	129.479	64.853	64.626	182.17	182.273
CBCT OC (9)	128.798	64.399	64.399	129.705	64.853	64.779	182.469	182.797
CBCT OC (10)	128.733	64.253	64.253	129.185	64.932	64.713	182.057	182.38
CBCT OL (1)	129.224	64.543	64.626	129.801	64.68	64.902	183.305	183.04
CBCT OL (2)	129.075	64.758	64.537	129.735	64.753	65.098	183.163	183.162
CBCT OL (3)	129.581	64.68	64.901	129.801	64.901	65.121	183.256	183.411
CBCT OL (4)	129.801	64.68	64.459	129.801	64.68	65.342	183.881	183.411
CBCT OL (5)	129.295	64.537	64.537	129.736	64.758	64.978	183.01	183.163
CBCT OL (6)	129.043	64.356	64.226	129.373	64.356	64.256	182.962	182.962
CBCT OL (7)	129.801	64.9	64.9	129.801	64.569	64.9	183.368	183.332
CBCT OL (8)	128.429	64.016	64.215	129.225	64.215	64.811	182.613	182.47
CBCT OL (9)	128.486	64.343	64.542	129.084	64.343	64.84	182.412	182.27
CBCT OL (10)	128.685	64.343	64.343	129.283	64.243	64.919	182.836	182.553

APPENDIX B

CLINICAL DATA COLLECTION – SIRONA

Patient #	**501**	**502**	**503**	**504**	**505**	**506**	**507**	**508**	**509**
I-I Angle	127.7	139.2	117.8	132.7	119.5	121.7	142.4	122.6	161.8
U1 Prot	6.6	2.4	7.1	4.8	10.0	6.4	4.4	6.4	1.9
L1 Prot	3.0	5.7	3.2	2.0	6.2	3.8	1.3	3.6	-1.3
L1 to APo	22.9	21.4	25.7	26.9	25.9	23.9	18.3	27.4	12.2
U6 - PTV	18.5	22.0	19.7	23.7	15.0	22.6	20.8	16.7	20.8
Convexity	3.6	-2.9	4.8	2.0	8.8	4.5	2.8	1.1	2.5
Mnd Arc	41.5	47.0	40.9	41.4	25.3	31.6	46.4	35.1	28.4
MPA	21.3	16.9	21.8	22.3	34.6	23.1	14.8	17.5	24.8
Mx Depth	94.4	86.9	93.2	90.5	95.9	95.6	95.5	88.6	93.9
F-Axis	88.5	89.2	86.3	86.3	82.1	89.9	88.1	92.9	89.5
F-Depth	90.8	89.3	88.7	88.4	87.1	91.1	92.8	87.3	91.2
C-Length	55.0	58.9	59.6	58.6	55.3	60.1	54.1	57.3	53.6
C-Def	30.1	27.1	29.4	31.2	31.5	29.8	32.3	27.9	29.0
LFH	42.5	38.8	46.2	43.9	50.7	47.6	39.9	43.4	51.5
LL-E	0.5	1.1	-2.0	-4.4	5.4	-0.8	0.1	-3.7	-3.5
N-Me	105.5	118.7	117.6	109.4	106.4	113.7	105.8	91.9	102.4
N-Ba	104.7	102.4	109.0	100.5	97.8	106.9	102.3	100.2	98.0

Clinical Data Collection – Sirona. *Continued*.

Patient #	**510**	**511**	**512**	**513**	**514**	**515**	**516**	**517**	**518**
I-I Angle	115.0	128.0	132.0	130.0	99.0	110.7	122.6	121.8	123.7
U1 Prot	8.4	6.1	6.1	8.5	8.8	9.4	8.2	5.0	2.4
L1 Prot	5.7	2.7	2.9	4.1	5.7	7.1	4.0	1.8	0.0
L1 to APo	33.3	26.3	23.2	24.8	39.3	28.4	25.0	24.4	32.5
U6 - PTV	9.8	15.6	18.2	18.8	22.2	16.1	17.9	18.7	13.1
Convexity	5.7	3.9	2.1	4.9	2.6	0.4	2.3	10.9	0.5
Mnd Arc	32.3	35.7	34.5	35.7	38.5	28.8	31.3	36.2	39.9
MPA	31.7	16.4	22.1	23.2	15.4	23.7	23.3	24.6	23.1
Mx Depth	88.0	97.0	89.0	94.8	95.4	89.4	93.6	95.2	88.2
F-Axis	77.1	92.7	88.3	87.4	90.4	92.5	93.4	84.1	86.4
F-Depth	83.0	93.0	87.1	90.0	92.9	89.0	91.0	85.0	87.7
C-Length	52.5	52.3	62.9	59.1	55.4	57.7	56.0	56.9	56.4
C-Def	29.4	28.9	29.0	30.3	30.7	27.4	27.9	29.6	29.0
LFH	52.0	40.4	42.8	47.2	41.3	42.0	41.4	44.3	43.1
LL-E	2.2	-0.6	-2.8	-0.1	-2.5	4.8	1.0	-1.2	-3.8
N-Me	113.2	95.7	111.0	114.1	106.5	98.1	97.8	105.2	107.3
N-Ba	96.6	94.3	107.7	105.7	99.6	98.5	96.5	101.4	99.0

Clinical Data Collection – Sirona. ***Continued.***

Patient #	**519**	**520**	**521**	**522**	**523**	**524**	**525**
I-I Angle	125.3	132.4	110.8	141.4	144.1	136.7	124.7
U1 Prot	3.5	4.7	9.4	2.1	5.1	6.1	4.1
L1 Prot	0.4	1	3.5	0	-0.5	2.1	2.4
L1 to APo	23	16.5	29	19.1	13.5	19.3	27.9
U6 - PTV	22.6	20	14.6	13	18.8	19.0	21.2
Convexity	8.6	3.3	4.3	1.3	5.6	3.7	-1.8
Mnd Arc	36.5	34.3	35.5	39.7	40.7	29.6	32.3
MPA	16.3	20.6	20.4	18.3	15.6	25.8	16.0
Mx Depth	99.3	95.1	93.2	90.5	96.6	93.9	92.8
F-Axis	90	86.1	89.4	93.6	89.6	87.4	96.4
F-Depth	92.5	92	88.9	89	90.8	90.0	94.9
C-Length	61.1	53.5	53.2	51.5	55.6	53.9	55.9
C-Def	30.8	32.9	28.1	25.6	32.4	30.3	30.8
LFH	43.2	42.2	44.8	39.7	35.1	45.3	37.3
LL-E	-3.0	-5.2	0.5	-3.9	-2.5	0.3	-2.7
N-Me	115.0	105.5	100	91.4	96.2	103.2	92.0
N-Ba	110.1	92.6	95.5	92.9	99.7	100.2	100.6

APPENDIX C

CLINICAL DATA COLLECTION – CBCT ORTHOGONAL 100%

Patient #	**501**	**502**	**503**	**504**	**505**	**506**	**507**	**508**	**509**
I-I Angle	127.7	139.4	117.1	132.4	120.4	122	142.5	122.2	161.8
U1 Prot	6.3	1.7	7.3	4.3	10.6	6.1	4	6.3	1.9
L1 Prot	2.6	5.4	3.6	1.4	6.4	3.8	1.2	3.4	-1.1
L1 to APo	23.9	19.8	27.4	27.5	27.0	24.9	19.3	26.4	13.1
U6 - PTV	18.0	21.4	17.7	22.1	14.0	21.8	19.9	16	20.6
Convexity	3.7	-2.7	4.5	1.8	8.4	4.1	2.4	1	2.1
Mnd Arc	39.4	47.0	37.7	40.5	26.9	35.7	43.4	35.7	30.3
MPA	19.5	16.6	22.6	22.8	35.3	23.6	15.6	17.9	25.9
Mx Depth	94.2	86.5	93.2	89.8	95.5	96.4	95.5	88.2	93
F-Axis	87.9	88.1	85.0	85.8	81.5	87.5	89	90	88.1
F-Depth	90.6	88.8	89.1	88.0	86.9	91.8	93.2	87.1	90.7
C-Length	54.9	58.3	57.7	56.0	52.5	56.1	53.9	55.2	53.3
C-Def	31.1	27.6	30.4	31.0	30.5	31	31.8	29.4	29.5
LFH	41.1	37.8	45.8	43.7	49.8	47.5	38.7	42.6	51.3
LL-E	-0.8	0.0	-1.4	-3.3	5.5	-1.8	-0.4	-2	-4.7
N-Me	103.2	117.7	116.4	105.4	105.4	112.9	105.8	91.8	102.2
N-Ba	102.8	102.7	106.7	97.7	95.8	104.3	101.9	98.7	96.4

Clinical Data Collection – Cbct Orthogonal 100%. *Continued.*

Patient #	**510**	**511**	**512**	**513**	**514**	**515**	**516**	**517**	**518**
I-I Angle	116	128.5	131.9	130.9	99.6	110.2	122	122.4	123.8
U1 Prot	8	5.8	5.8	8.4	8.2	9.2	8	5.7	2.3
L1 Prot	4.7	2.4	2.9	3.7	5.6	6.6	3.5	2.8	-0.3
L1 to APo	30.5	25.2	24.3	23.7	40.7	28.9	24.9	25.5	33.8
U6 - PTV	9.2	15.2	17.4	18	21.4	15.3	16.5	18	13.5
Convexity	6.4	4.1	1.8	4.4	2.3	0.1	2.3	10.2	0.1
Mnd Arc	31.1	34.9	32.9	36.6	37	27.3	34.9	36.1	37.4
MPA	30.1	16.9	23.5	24.7	15.9	23.8	24.1	25	22.9
Mx Depth	88.3	96.7	87.9	94.1	95.4	89.2	92.9	94.3	88.1
F-Axis	77.2	92.3	88	85.2	89.7	92.5	91.9	84.4	86.3
F-Depth	82.6	92.5	86.2	89.8	93.2	89.1	90.2	84.6	88
C-Length	50.9	51.5	61.5	58.6	54.3	53.9	53.4	57.2	57.5
C-Def	28.8	28.8	28.5	31.7	31.6	26	27.8	29.4	30
LFH	52.3	41.5	42.2	47.7	41.1	44.3	40.4	43.7	43.8
LL-E	1.2	-0.5	-3	0.2	-1.9	3.8	0.5	-0.9	-3.9
N-Me	112.3	94.4	108.5	113	104.4	97	96.1	104.7	107.2
N-Ba	95	92.2	106.5	103.2	97.8	97.6	94.4	101	98.8

Clinical Data Collection – Cbct Orthogonal 100%. *Continued.*

Patient #	**519**	**520**	**521**	**522**	**523**	**524**	**525**
I-I Angle	125.2	132.3	110.9	141.8	143.5	136.5	126.2
U1 Prot	3.8	4.7	9	1.7	4.9	6.1	4
L1 Prot	0.1	0.8	3.2	-0.4	-0.7	2	2
L1 to APo	23.3	18.2	29.6	17.1	14.2	18.9	27.1
U6 - PTV	21.1	19.5	14	12.5	18.3	18.7	20.6
Convexity	7.7	3	4.1	1.2	5.2	3.9	-2
Mnd Arc	37.1	36.6	33.6	40.6	39.7	29.4	34.8
MPA	17.5	21	20.1	16.4	14.3	26.9	15.4
Mx Depth	98.8	94.9	93.8	90.8	97.2	93.1	92.4
F-Axis	89.7	86.4	89.8	93	87.9	87	97
F-Depth	92	92	89.6	89.4	91.9	88.9	94.8
C-Length	60.1	52.5	51.5	50.9	54.3	52.7	56.1
C-Def	30.7	32.5	27.5	26.6	34.9	29.1	30.5
LFH	43.2	41.3	43.6	40.8	35.2	46.4	37
LL-E	-4.7	-4.5	0.7	-3.8	-1	0.6	-4.6
N-Me	112.7	104.4	99.2	90.7	95.4	102.5	91.7
N-Ba	108.3	91.6	93.8	91.8	99.1	99	100.7

APPENDIX D

CLINICAL DATA COLLECTION – CBCT ORTHOGONAL 101%

Patient #	**501**	**502**	**503**	**504**	**505**	**506**	**507**	**508**	**509**
I-I Angle	127.7	139.4	117.1	132.4	120.4	122	142.5	122.2	161.8
U1 Prot	6.4	1.7	7.4	4.4	10.7	6.1	4	6.3	1.9
L1 Prot	2.6	5.4	3.6	1.4	6.5	3.9	1.2	3.4	-1.2
L1 to APo	23.9	19.8	27.4	27.5	27	24.9	19.3	26.4	13.1
U6 - PTV	18.2	21.7	17.9	22.3	14.1	22	20.1	16.2	20.8
Convexity	3.8	-2.8	4.5	1.8	8.5	4.6	2.4	1	2.2
Mnd Arc	39.4	47.1	37.7	40.5	26.9	35.7	43.4	35.7	30.3
MPA	19.5	16.6	22.6	22.8	35.3	23.6	15.6	17.9	25.9
Mx Depth	94.2	86.6	93.2	89.8	95.5	96.4	95.5	88.2	93
F-Axis	87.9	88.1	85.0	85.8	81.5	87.5	89	90	88.1
F-Depth	90.6	88.9	89.1	88.0	86.9	91.8	93.2	87.1	90.7
C-Length	55.5	58.9	58.3	56.6	53	56.7	54.4	55.7	53.9
C-Def	31.1	27.6	30.4	31.0	30.5	31	31.8	29.4	29.5
LFH	41.1	37.8	45.8	43.7	49.8	47.5	38.7	42.6	51.3
LL-E	-0.8	0.0	-1.4	-3.4	5.5	-1.8	-0.4	-2.1	-4.8
N-Me	104.3	118.9	117.5	106.5	106.5	114	106.9	92.7	103.2
N-Ba	103.8	103.7	107.8	99.5	96.8	105.4	102.9	99.7	97.3

Clinical Data Collection – Cbct Orthogonal 101%. *Continued.*

Patient #	**510**	**511**	**512**	**513**	**514**	**515**	**516**	**517**	**518**
I-I Angle	116	128.5	131.9	130.9	99.6	110.2	122	122.4	123.8
U1 Prot	8.1	5.8	5.8	8.5	8.3	9.3	8.1	5.8	2.3
L1 Prot	4.8	2.5	2.9	3.7	5.6	6.7	3.5	2.8	-0.3
L1 to APo	30.5	25.2	24.3	23.7	40.7	28.9	24.9	25.5	33.8
U6 - PTV	9.3	15.4	17.6	18.2	21.7	15.4	16.7	18.2	13.7
Convexity	6.4	4.1	1.8	4.4	2.3	0.1	2.4	10.3	0.1
Mnd Arc	31.1	34.9	32.9	36.6	37	27.3	34.9	36.1	37.4
MPA	30.1	16.9	23.5	24.7	15.9	23.8	24.1	25	22.9
Mx Depth	88.3	96.7	87.9	94.1	95.4	89.2	92.9	94.3	88.1
F-Axis	77.2	92.3	88	85.2	89.7	92.5	91.9	84.4	86.3
F-Depth	82.6	92.5	86.2	89.8	93.2	89.1	90.2	84.6	88
C-Length	51.4	52	62.1	59.2	54.8	54.5	53.9	57.8	58.1
C-Def	28.8	28.8	28.5	31.7	31.6	26	27.8	29.4	30
LFH	52.3	41.5	42.2	47.7	41.1	44.3	40.4	43.7	43.8
LL-E	1.2	-0.5	-3.1	0.2	-1.9	3.8	0.5	-0.9	-4
N-Me	113.4	95.3	109.6	114.1	105.4	97.9	97	105.8	108.3
N-Ba	96	93.1	107.6	104.2	98.8	98.6	95.3	102	99.8

Clinical Data Collection – Cbct Orthogonal 101%. *Continued.*

Patient #	**519**	**520**	**521**	**522**	**523**	**524**	**525**
I-I Angle	125.2	132.3	110.9	141.8	143.5	136.5	126.2
U1 Prot	3.8	4.8	9.1	1.7	5	6.1	4.1
L1 Prot	0.1	0.8	3.2	-0.4	-0.7	2	2
L1 to APo	23.3	18.2	29.6	17.1	14.2	18.9	27.1
U6 - PTV	21.3	19.7	14.1	12.6	18.4	18.9	20.8
Convexity	7.8	3	4.2	1.3	5.3	3.9	-2.1
Mnd Arc	37.1	36.6	33.6	40.6	39.7	29.4	34.8
MPA	17.5	21	20.1	16.4	14.3	26.9	15.4
Mx Depth	98.8	94.9	93.8	90.8	97.2	93.1	92.4
F-Axis	89.7	86.4	89.8	93	87.9	87	97
F-Depth	92	92	89.6	89.4	91.9	88.9	94.8
C-Length	60.7	53	52	51.4	54.9	53.3	56.7
C-Def	30.7	32.5	27.5	26.6	34.9	29.1	30.5
LFH	43.2	41.3	43.6	40.8	35.2	46.4	37
LL-E	-4.8	-4.6	0.7	-3.8	-1	0.6	-4.6
N-Me	113.9	105.4	100.2	91.6	96.4	103.6	92.6
N-Ba	109.3	92.6	94.8	92.7	100.1	100	101.7

APPENDIX E

CLINICAL DATA COLLECTION – CBCT ORTHOGONAL 102%

Patient #	**501**	**502**	**503**	**504**	**505**	**506**	**507**	**508**	**509**
I-I Angle	127.7	139.4	117.1	132.4	120.4	122	142.5	122.2	161.8
U1 Prot	6.4	1.8	7.4	4.4	10.8	6.2	4.1	6.4	1.9
L1 Prot	2.7	5.5	3.7	1.4	6.5	3.9	1.2	3.4	-1.2
L1 to APo	23.9	19.8	27.4	27.5	27	24.9	19.3	26.4	13.1
U6 - PTV	18.4	21.9	18.1	22.5	14.2	22.3	20.3	16.3	21
Convexity	3.8	-2.8	4.6	1.8	8.5	4.6	2.4	1	2.2
Mnd Arc	39.4	47.1	37.7	40.5	26.9	35.7	43.4	35.7	30.3
MPA	19.5	16..6	22.6	22.8	35.3	23.6	15.6	17.9	25.9
Mx Depth	94.2	86.6	93.2	89.8	95.5	96.4	95.5	88.2	93
F-Axis	87.9	88.2	85.0	85.8	81.5	87.5	89	90	88.1
F-Depth	90.6	88.9	89.1	88.0	86.9	91.8	93.2	87.1	90.7
C-Length	56	59.4	58.9	57.2	53.5	57.2	54.9	56.3	54.4
C-Def	31.1	27.6	30.4	31.0	30.5	31	31.8	29.4	29.5
LFH	41.1	37.8	45.8	43.7	49.8	47.5	38.7	42.6	51.3
LL-E	-0.8	0.0	-1.4	-3.4	5.6	-1.8	-0.4	-2.1	-4.8
N-Me	105.3	120.1	118.7	107.5	107.6	115.1	107.9	93.6	104.2
N-Ba	104.9	104.8	108.8	100.5	97.8	106.4	103.9	100.7	98.3

Clinical Data Collection – Cbct Orthogonal 102%. *Continued.*

Patient #	**510**	**511**	**512**	**513**	**514**	**515**	**516**	**517**	**518**
I-I Angle	116	128.5	131.9	130.9	99.6	110.2	122	122.4	123.8
U1 Prot	8.2	5.9	5.9	8.6	8.3	9.4	8.2	5.8	2.4
L1 Prot	4.8	2.5	2.9	3.8	5.7	6.7	3.6	2.8	-0.3
L1 to APo	30.5	25.2	24.3	23.7	40.7	28.9	24.9	25.5	33.8
U6 - PTV	9.4	15.5	17.8	18.4	21.9	15.6	16.8	18.4	13.8
Convexity	6.5	4.2	1.8	4.5	2.3	0.1	2.4	10.4	0.1
Mnd Arc	31.1	34.9	32.9	36.6	37	27.3	34.9	36.1	37.4
MPA	30.1	16.9	23.5	24.7	15.9	23.8	24.1	25	22.9
Mx Depth	88.3	96.7	87.9	94.1	95.4	89.2	92.9	94.3	88.1
F-Axis	77.2	92.3	88	85.2	89.7	92.5	91.9	84.4	86.3
F-Depth	82.6	92.5	86.2	89.8	93.2	89.1	90.2	84.6	88
C-Length	52	52.5	62.7	59.8	55.3	55	54.4	58.3	58.7
C-Def	28.8	28.8	28.5	31.7	31.6	26	27.8	29.4	30
LFH	52.3	41.5	42.2	47.7	41.1	44.3	40.4	43.7	43.8
LL-E	1.2	-0.5	-3.1	0.2	-1.9	3.9	0.6	-1	-4
N-Me	114.6	96.2	110.7	115.2	106.4	98.9	98	106.8	109.3
N-Ba	96.9	94	108.7	105.3	99.8	99.6	96.3	103	100.8

Clinical Data Collection – Cbct Orthogonal 102%. *Continued.*

Patient #	**519**	**520**	**521**	**522**	**523**	**524**	**525**
I-I Angle	125.2	132.3	110.9	141.8	143.5	136.5	126.2
U1 Prot	3.8	4.8	9.2	1.8	5	6.2	4.1
L1 Prot	0.1	0.8	3.2	-0.4	-0.7	2	2.1
L1 to APo	23.3	18.2	29.6	17.1	14.2	18.9	27.1
U6 - PTV	21.5	19.9	14.3	12.8	18.6	19	21
Convexity	7.8	3	4.2	1.3	5.3	4	-2.1
Mnd Arc	37.1	36.6	33.6	40.6	39.7	29.4	34.8
MPA	17.5	21	20.1	16.4	14.3	26.9	15.4
Mx Depth	98.8	94.9	93.8	90.8	97.2	93.1	92.4
F-Axis	89.7	86.4	89.8	93	87.9	87	97
F-Depth	92	92	89.6	89.4	91.9	88.9	94.8
C-Length	61.3	53.5	52.5	51.9	55.4	53.8	57.2
C-Def	30.7	32.5	27.5	26.6	34.9	29.1	30.5
LFH	43.2	41.3	43.6	40.8	35.2	46.4	37
LL-E	-4.8	-4.6	0.7	-3.9	-1	0.6	-4.7
N-Me	115	106.5	101.2	92.5	97.3	104.6	93.5
N-Ba	110.4	93.5	95.7	93.6	101.1	101	102.7

APPENDIX F

CLINICAL DATA COLLECTION – CBCT ORTHOGONAL 103%

Patient #	**501**	**502**	**503**	**504**	**505**	**506**	**507**	**508**	**509**
I-I Angle	127.7	139.4	117.1	132.4	120.4	122	142.5	122.2	161.8
U1 Prot	6.5	1.8	7.5	4.4	10.9	6.3	4.1	6.4	1.9
L1 Prot	2.7	5.5	3.7	1.4	6.6	3.9	1.2	3.5	-1.2
L1 to APo	23.9	19.8	27.4	27.5	27	24.9	19.3	26.4	13.1
U6 - PTV	18.6	22.1	18.3	22.8	14.4	22.5	20.5	16.5	21.2
Convexity	3.8	-2.8	4.6	1.8	8.6	4.7	2.5	1	2.2
Mnd Arc	39.4	47.1	37.7	40.5	26.9	35.7	43.4	35.7	30.3
MPA	19.5	16..8	22.6	22.8	35.3	23.6	15.6	17.9	25.9
Mx Depth	94.2	86.6	93.2	89.8	95.5	96.4	95.5	88.2	93
F-Axis	87.9	88.2	85.0	85.8	81.5	87.5	89	90	88.1
F-Depth	90.6	88.9	89.1	88.0	86.9	91.8	93.2	87.1	90.7
C-Length	56.6	60.0	59.5	57.7	54.1	57.8	55.5	56.8	54.9
C-Def	31.1	27.6	30.4	31.0	30.5	31	31.8	29.4	29.5
LFH	41.1	37.8	45.8	43.7	49.8	47.5	38.7	42.6	51.3
LL-E	-0.8	0.0	-1.4	-3.4	5.6	-1.8	-0.4	-2.1	-4.9
N-Me	106.3	121.2	119.9	108.6	108.6	116.3	109	94.5	105.5
N-Ba	105.9	105.8	109.9	101.5	98.7	107.5	104.9	101.6	99.3

Clinical Data Collection – Cbct Orthogonal 103%. *Continued.*

Patient #	**510**	**511**	**512**	**513**	**514**	**515**	**516**	**517**	**518**
I-I Angle	116	128.5	131.9	130.9	99.6	110.2	122	122.4	123.8
U1 Prot	8.3	6	5.9	8.6	8.4	9.5	8.3	5.9	2.4
L1 Prot	4.9	2.5	3	3.8	5.8	6.8	3.6	2.9	-0.3
L1 to APo	30.5	25.2	24.3	23.7	40.7	28.9	24.9	25.5	33.8
U6 - PTV	9.5	15.7	18	18.5	22.1	15.7	17	18.6	13.9
Convexity	6.6	4.2	1.9	4.5	2.4	0.1	2.4	10.5	0.1
Mnd Arc	31.1	34.9	32.9	36.6	37	27.3	34.9	36.1	37.4
MPA	30.1	16.9	23.5	24.7	15.9	23.8	24.1	25	22.9
Mx Depth	88.3	96.7	87.9	94.1	95.4	89.2	92.9	94.3	88.1
F-Axis	77.2	92.3	88	85.2	89.7	92.5	91.9	84.4	86.3
F-Depth	82.6	92.5	86.2	89.8	93.2	89.1	90.2	84.6	88
C-Length	52.5	53	63.3	60.4	55.9	55.6	55	58.9	59.3
C-Def	28.8	28.8	28.5	31.7	31.6	26	27.8	29.4	30
LFH	52.3	41.5	42.2	47.7	41.1	44.3	40.4	43.7	43.8
LL-E	1.1	-0.5	-3.1	0.2	-1.9	3.9	0.6	-1	-4.1
N-Me	115.7	97.2	111.8	116.4	107.5	99.9	99	107.9	110.4
N-Ba	97.9	94.9	109.7	106.3	100.7	100.6	97.2	104	101.8

Clinical Data Collection – Cbct Orthogonal 103%. *Continued.*

Patient #	**519**	**520**	**521**	**522**	**523**	**524**	**525**
I-I Angle	132.2	110.9	141.8	143.5	136.5	126.2	132.2
U1 Prot	4.9	9.3	1.8	5.1	6.3	4.1	4.9
L1 Prot	0.8	3.3	-0.4	-0.7	2.1	2.1	0.8
L1 to APo	18.2	29.6	17.1	14.2	18.9	27.1	18.2
U6 - PTV	20.1	14.4	12.9	18.8	19.2	21.2	20.1
Convexity	3.1	4.3	1.3	5.4	4	-2.1	3.1
Mnd Arc	36.6	33.6	40.6	39.7	29.4	34.8	36.6
MPA	21	20.1	16.4	14.3	26.9	15.4	21
Mx Depth	94.9	93.8	90.8	97.2	93.1	92.4	94.9
F-Axis	86.4	89.8	93	87.9	87	97	86.4
F-Depth	92	89.6	89.4	91.9	88.9	94.8	92
C-Length	54	53	52.4	56	54.3	57.8	54
C-Def	32.5	27.5	26.6	34.9	29.1	30.5	32.5
LFH	41.3	43.6	40.8	35.2	46.4	37	41.3
LL-E	-4.6	0.7	-3.9	-1.1	0.6	-4.7	-4.6
N-Me	107.5	102.2	93.4	98.3	105.6	94.4	107.5
N-Ba	94.4	96.6	94.6	102.1	102	103.7	94.4

APPENDIX G

CLINICAL DATA COLLECTION – CBCT PERSPECTIVE

Patient #	**501**	**502**	**503**	**504**	**505**	**506**	**507**	**508**	**509**
I-I Angle	128.3	139.4	116.7	132.4	120.6	122.4	141.6	121.6	161.5
U1 Prot	7.1	2.5	8.1	4.4	11.6	6.8	4.2	7.0	2.9
L1 Prot	3.2	6.5	4.4	1.4	7.2	3.8	1.0	3.7	-0.3
L1 to APo	23.9	19.5	26.4	27.5	26.2	22.9	19.5	25.6	10.7
U6 - PTV	19.6	25.1	19.3	23.6	15.6	24.0	22.1	17.1	22.6
Convexity	4.1	-3.5	5.2	2.0	9.6	5.1	3.2	1.4	2.3
Mnd Arc	39.7	47.5	39.4	38.6	24.0	33.5	44.1	35.5	30.0
MPA	19.7	16.3	22.2	23.6	35.1	22.4	14.5	17.9	24.7
Mx Depth	93.8	85.9	93.5	89.3	95.2	95.8	95.8	88.1	93.0
F-Axis	87.1	89.5	86.7	85.9	81.1	88.2	89.2	90.6	87.9
F-Depth	90.1	88.5	89.1	87.4	86.3	91.1	93.0	86.7	90.6
C-Length	59.5	66.2	63.8	63.8	58.8	62.7	58.7	59.5	57.7
C-Def	30.9	27.0	29.1	30.9	30.7	30.1	31.7	28.3	29.3
LFH	41.2	38.2	45.8	43.6	50.8	47.3	39.3	42.9	51.6
LL-E	-0.4	0.5	-1.5	-3.7	6.2	-2.2	0.3	-2.3	-5.3
N-Me	113.4	128.6	128.0	117.3	116.4	123.7	114.4	99.8	114.1
N-Ba	113.2	111.8	117.5	107.8	105.1	114.8	110.6	107.4	107.3

Clinical Data Collection – Cbct Perspective. ***Continued.***

Patient #	**510**	**511**	**512**	**513**	**514**	**515**	**516**	**517**	**518**
I-I Angle	116.5	128.4	131.6	130.6	99.2	110.7	121.9	122.0	123.6
U1 Prot	9.6	6.8	7.2	9.0	9.1	10.6	8.8	6.6	2.6
L1 Prot	6.3	2.9	3.2	3.9	6.4	7.6	4.6	2.8	0.0
L1 to APo	33.2	26.5	25.2	23.5	39.5	29.4	25.1	25.0	32.0
U6 - PTV	10.3	16.9	19.5	19.7	23.1	15.4	18.7	18.8	14.8
Convexity	5.7	4.3	1.8	6.0	2.9	0.1	2.7	11.8	0.7
Mnd Arc	32.6	36.2	32.5	37.2	35.9	29.0	35.0	37.8	38.6
MPA	30.5	16.9	24.0	24.8	14.3	23.8	23.9	24.9	22.2
Mx Depth	87.5	97.8	88.1	94.5	96.1	88.8	92.7	95.2	88.9
F-Axis	77.4	92.4	88.3	87.7	89.2	92.4	92.6	83.6	86.2
F-Depth	82.6	93.6	86.5	89.2	93.6	88.7	89.9	84.9	88.3
C-Length	57.0	57.2	67.2	65.1	58.6	58.7	60.1	62.0	62.5
C-Def	29.1	30.2	28.1	29.3	32.0	25.6	27.6	29.8	30.1
LFH	53.5	41.1	43.7	46.9	42.1	43.1	40.9	42.9	44.1
LL-E	2.2	-1.2	-3.8	0.0	-2.3	3.3	0.6	-0.7	-4.1
N-Me	122.3	103.1	119.1	123.2	114.6	104.9	105.6	115.3	117.4
N-Ba	104.2	101.5	114.9	108.2	107.1	105.7	103.8	111.3	108.6

Clinical Data Collection – Cbct Orthogonal 103%. *Continued.*

Patient #	**519**	**520**	**521**	**522**	**523**	**524**	**525**
I-I Angle	124.5	131.9	110.6	141.4	143.6	135.6	126.9
U1 Prot	4.6	5.4	10.2	2.1	5.9	7.1	4.3
L1 Prot	0.4	1.5	3.8	0.2	0.4	2.7	2.3
L1 to APo	23.2	18	29.4	17.5	14.1	20	25.9
U6 - PTV	24.7	20.5	15.5	14.2	19.9	20.2	22.6
Convexity	8	3.7	5.2	1.8	5.5	4.4	-1.8
Mnd Arc	37.1	39.3	34.7	38.2	39.3	28.2	34.8
MPA	16.1	21.5	21	17.2	14.4	27.9	15.1
Mx Depth	99	94.7	94.4	91.1	96.3	94.1	92.8
F-Axis	89.4	86.4	89.1	94.1	86.9	87.3	97.3
F-Depth	92.4	91.5	89.6	89.2	91.3	89.8	94.7
C-Length	65.2	58.5	57.3	54.6	61.7	57.4	62.6
C-Def	31.4	32	28.5	25.2	34.7	29.4	30.4
LFH	42.9	41.1	43.8	40.9	36.2	46.2	37.5
LL-E	-4.4	-5.3	0.9	-4.5	-1.5	0.8	-4.9
N-Me	122.3	116.1	109.2	98	108.8	112	100.9
N-Ba	118.2	102.6	103.8	100.5	111.8	107.4	111.0

APPENDIX H

REPEATED CLINICAL DATA MEASUREMENTS BY TWO EXAMINERS

Patient #	**501 Y.J.1**	**501 Y.J.2**	**501 Y.J.3**	**501 L.L.**	**502 Y.J.1**	**502 Y.J.2**	**502 Y.J.3**	**502 L.L.**
I-I Angle	130.6	126.3	128.7	126.9	139.2	138.0	141.3	136.8
U1 Prot	7.0	6.4	6.6	6.6	2.4	3.6	3.3	2.7
L1 Prot	4.0	3.6	4.1	3.7	5.7	7.0	7.2	5.5
L1 to APo	22.1	24.2	24.9	25.0	21.4	21.8	21.6	20.2
U6 - PTV	18.5	17.8	17.9	17.0	22.0	23.9	22.8	21.7
Convexity	4.1	3.7	2.2	3.4	-2.9	-3.5	-3.8	-2.7
Mnd Arc	42.9	39.8	38.6	37.4	47.0	46.2	44.3	43.6
MPA	21.3	19.4	18.9	22.6	16.9	12.5	14	15.5
Mx Depth	94.9	94.2	93.0	93.0	86.9	86.8	84.9	89.1
F-Axis	88.5	88.4	89.2	89.9	89.2	88.0	88.8	90.2
F-Depth	90.8	90.5	90.9	89.6	89.3	90.6	89.2	89.2
C-Length	55.0	55.3	56.1	56.0	58.9	58.2	59.7	60.4
C-Def	30.1	30.1	29.8	29.0	27.0	29.3	27.6	27.2
LFH	41.2	41.6	42.8	41.6	38.8	40.5	39.7	37.8
LL-E	0.5	1.0	0.1	0.4	1.1	1.7	1.1	1.7
N-Me	105.5	105.9	106.6	103.4	118.7	118.7	119.1	117.3
N-Ba	104.7	105.4	106.5	102.7	102.4	103.2	103.8	99.7

Repeated Clinical Data Measurements By Two Examiners. *Continued.*

Patient #	**503 Y.J.1**	**503 Y.J.2**	**503 Y.J.3**	**503 L.L.**	**504 Y.J.1**	**504 Y.J.2**	**504 Y.J.3**	**504 L.L.**
I-I Angle	116.3	119.0	117.4	111.9	132.1	128.3	129.6	127.7
U1 Prot	7.5	8.2	8.0	8.9	4.5	4.4	4.8	5.3
L1 Prot	4.1	4.8	4.1	5.2	1.1	1.7	2.3	2.4
L1 to APo	28.2	26.4	27.7	28.7	24.3	31.8	31.0	29.3
U6 - PTV	19.7	18.5	18.9	17.8	23.2	24.9	24.3	21.9
Convexity	4.9	3.9	4.3	3.1	2.6	1.6	1.5	2.1
Mnd Arc	40.6	35.7	36.5	38.2	36.8	38.9	39.1	34.2
MPA	21.4	20.6	21.1	23.3	25.8	24.9	25.4	29.7
Mx Depth	93.5	93.1	93.9	92.4	90.4	90.5	90.2	89.0
F-Axis	87.3	86.6	87.1	86.4	87.3	88.4	87.4	87.6
F-Depth	89.0	89.5	89.8	89.3	87.9	88.9	88.7	86.8
C-Length	59.1	60.3	60.5	58.9	58.5	58.7	58.0	56.0
C-Def	28.7	30.2	29.9	30.2	29.4	29.7	30.1	27.9
LFH	46.5	47.8	47.6	48.3	44.7	44.2	43.8	44.8
LL-E	-2.0	-2.0	-2.6	0.6	-4.4	-3.9	-4.9	-4.9
N-Me	117.8	118.9	118.7	116.3	109.4	108.6	108.6	105.4
N-Ba	109.0	110.4	109.7	107.9	100.5	97.6	98.8	95

Repeated Clinical Data Measurements By Two Examiners. *Continued.*

Patient #	**505 Y.J.1**	**505 Y.J.2**	**505 Y.J.3**	**505 L.L.**
I-I Angle	117.0	117.7	118.1	117.5
U1 Prot	10.0	10.4	10.3	10.0
L1 Prot	6.2	6.4	6.6	5.8
L1 to APo	27.3	27.0	25.1	24.9
U6 - PTV	14.3	14.4	13.7	12.1
Convexity	8.9	8.2	8.6	8.7
Mnd Arc	24.5	24.2	25.2	19.9
MPA	34.1	34.9	36.4	38.1
Mx Depth	95.9	95.1	94.0	93.3
F-Axis	82.7	83.7	83.1	83.3
F-Depth	87.0	86.8	85.5	84.5
C-Length	54.8	55.4	55.6	53.5
C-Def	30.6	29.5	28.9	27.8
LFH	51.5	48.8	48.6	49.7
LL-E	5.4	5.5	5.8	6.5
N-Me	106.4	106.9	106.5	104.9
N-Ba	97.8	99.4	99.4	96.6